

NGC 4151 – A unified active galactic nucleus

I. Cassidy and D.J. Raine

Department of Physics and Astronomy, University of Leicester, Leicester, LE1 7RH, UK

Received 5 December 1995 / Accepted 31 October 1996

Abstract. We present a unified picture of active galactic nuclei which we construct from a detailed model of line emission in the active source in NGC 4151. This source provides us with an opportunity to explore the variation of structure with luminosity in an object which, in the model, derives its unusual properties as a consequence of the angle of the accretion disc to the line of sight. The key features that emerge from the model are (i) a non-spherical broad line region (BLR); (ii) short-lived BLR clouds; (iii) a luminosity-dependent structure for the BLR; (iv) a luminosity-dependent flared accretion disc extending beyond the BLR and (v) a separate intermediate line region between the BLR and NLR. The special orientation turns out to enable us to fix many of the parameters of the model for this source. It is then natural to ask how this model would appear, in its various luminosity states, at other orientations. To make contact with observations we need to include dust obscuration over a range of angles near to the plane of the disc. We then obtain the spread of observed types of radio-quiet active nuclei and we propose an extension of the model to a unification of radio-loud active galaxies. Thus, in this scheme NGC 4151 can be regarded as a typical active nucleus, special only in its orientation. We shall find that this alleviates a number of problems with a unified picture based on a dusty molecular torus with a fixed structure (to which NGC 4151 appears as an anomaly). In the proper sense of the expression, NGC 4151 may be the exception that proves the rule.

Key words: galaxies: active – nuclei – NGC 4151 – Seyfert-accretion, accretion disks

1. Introduction

In order to explain polarisation data for the radio galaxy 3C 234 Antonucci (1984) proposed a model in which the continuum source and broad-line clouds are located inside a thick torus, which blocks these from direct view, while electrons above and below the source scatter continuum and broad-line photons into the line of sight. This picture was extended following the discovery that the type 2 Seyfert galaxy NGC 1068 harbours a nucleus, of the same nature as a typical Seyfert type 1 nucleus, which

is hidden from direct view but which is revealed indirectly in scattered light. A model thus evolved of a partially obscuring dusty torus as a universal feature of Seyfert galaxies, in which observed differences are supposed to arise only from different lines of sight to intrinsically similar objects. The thickness of the torus and its opening angle are assumed to be independent of luminosity. Indeed, in the extreme hypothesis that Antonucci (1993) calls the straw person's model (SPM), the only difference amongst AGN is the division into radio-quiet and radio-loud types. The opening angle of the torus is then set by the observation of polarisation perpendicular to the radio axis in NGC 1068. Since a scattered photon retains a polarisation orthogonal to the propagation vector prior to scattering the bundle of ray directions before scattering cannot diverge too much. This gives a half-opening angle of at most 30° , consistent with the ratio of Seyfert type 1 to type 2 galaxies if the latter are all obscured views of the former.

But in schemes such as the SPM in which the structure proposed for NGC 1068 is typical, the active nucleus of NGC 4151 presents itself as a unique exception, essentially because the line of sight over the putative obscuring torus is incompatible with the view of the observed ionisation cone in the extended narrow line region (Penston et al. 1990; Evans et al. 1993) and possibly also the extended linear radio structure along the axis of the torus (Antonucci 1993).

The variation on the theme of unification that we present in this paper is, in contrast, based on a detailed analysis of NGC 4151. Our picture of this galaxy, which results from fitting emission line properties, is described in Cassidy & Raine (1996) and summarised in Sect. 2. We make the assumptions (i) that the accretion disc extends out to the BLR and (ii) that there is a supersonic nuclear wind generated close to the black hole. The BLR clouds arise from material injected from the accretion disc into the outflowing wind (Cassidy & Raine 1993). In the supersonic flow the BLR clouds are short-lived. Therefore the BLR is confined to a region close to the disc surface. This means that the BLR can respond rapidly to changes in the continuum, in contrast to a spherical BLR (Sect. 5.1). Thus if changes in the continuum result in a loss of BLR clouds, as we showed previously, a change of Seyfert type can occur on short timescales.

The dispersing cloud material provides a scattering medium by which the BLR and UV/optical continuum may be observed in systems where it is obscured from direct view. From other lines of sight this same material is the X-ray warm absorber. To account for the obscured systems we introduce a dusty torus in the region between the BLR and NLR, which may also be responsible for at least part of the IR emission (Efstathiou & Rowan-Robinson 1995). The non-spherical BLR geometry (and the location of the scattering medium) turns out to imply that the torus does not have to have a *small* opening angle. The existence of Seyfert 2 galaxies truly lacking a broad-line region, predicted by the model, takes care of the ratio of Seyfert types, which would otherwise be increased in favour of Seyfert 1s by the larger opening angle. This also provides a possible solution to the over-production of the X-ray background, because the number of obscured high luminosity Seyfert 1s is reduced.

The model itself determines differences in systems at lower and higher luminosities than the range covered in NGC 4151 and this is shown to account for the whole of the radio-quiet class of AGN. In particular, the obscuring torus is here part of a flared accretion disc and is located in a region where it may be influenced by the nuclear properties such that the opening angle increases with luminosity.

The following list of contents of the paper will serve to explain its structure. Sect. 2 reviews the basic features of our model for NGC 4151. In Sect. 2.1 we argue that the material from the dispersing broad-line clouds produces a medium that can provide a significant electron scattering optical depth to the continuum and broad-line emission. In Sect. 2.2 we show that, for other lines of sight, the dispersing cloud material also provides a warm absorber in the X-ray band. For NGC 4151 we show that the line of sight implies a combination of partial covering of the X-ray source by cold clouds and by this warm absorber, and show this prediction is consistent with Ginga X-ray data. We argue that the UV absorption may be explained without invoking any additional components in Sect. 2.3. Changes in the continuum illumination of the disc lead to suppression of the broad-line cloud production and in Sect. 3 we argue that this is consonant with the observed changes in broad-line properties in intermediate Seyferts. We predict the existence of true Seyfert 2 galaxies, lacking a broad-line region. In Sect. 4 we argue that the ‘unified Seyfert’ must contain an obscuring dusty torus, and that the presence of such a torus is consistent with the properties of NGC 4151 provided that the opening angle is sufficiently large. Having established the structure of NGC 4151 we investigate what it would look like at different angles. The importance of a flattened cloud geometry for the BLR is discussed in Sect. 5.1. The X-ray absorption is considered as a function of the angle of the disc to the line of sight in Sect. 5.2 The scattering into the line of sight of the obscured inner region at low inclinations is considered in Sect. 5.3. Arguments for the presence of an ILR in all higher luminosity AGN are considered in Sect. 5.4.

Sect. 6.1 deals with the flaring of the disc as a function of luminosity. We explain here why we consider the opening angle of the obscuring torus to be luminosity dependent. As a result, at low inclinations in high luminosity systems we predict broad

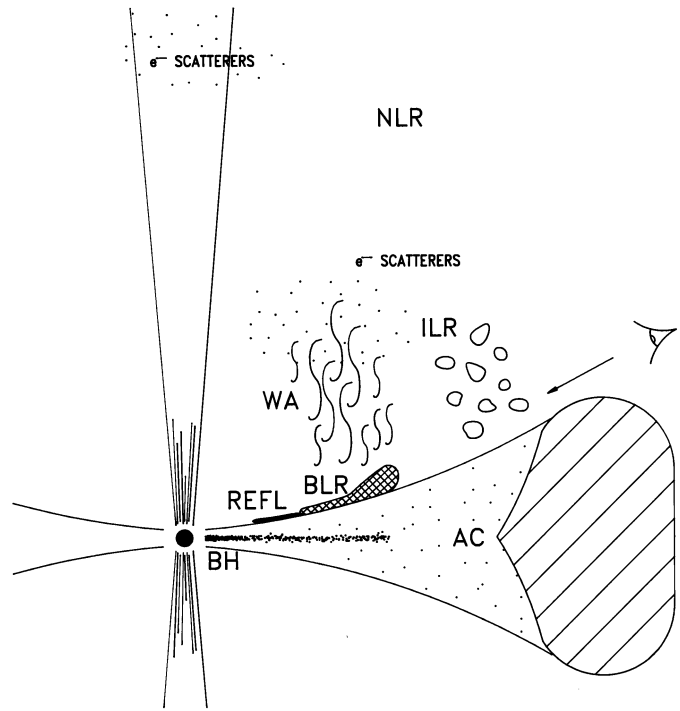


Fig. 1. Figure shows the structure of NGC 4151 including the warm absorber and reflector inferred from X-ray studies. We have a flared accretion disc with an optically thick, geometrically thin layer surrounding a black hole with either strong or weak radio jets. The flaring and thickness of the disc are, of course, luminosity dependent. The X-rays are created close to the black hole and are reflected by part of the inner accretion disc (Nandra et al. 1989). At distances $\geq 10^{16}$ cm broad-line clouds are formed. These clouds break up within two sound-crossing times and the cloud remnants form the warm absorber (WA). At distances $\geq 10^{18}$ cm the intermediate emission line clouds form. At distances $\geq 10^{19}$ cm we find the narrow line clouds, which are probably distributed isotropically.

absorption line quasars and explain why we believe this type of system will be radio-quiet. In the next sections we extend the model to lower luminosities (Sect. 6.2) and higher luminosities (Sect. 6.3). Finally, in Sect. 7, we discuss briefly how the model extends rather naturally to accommodate radio-loud objects in a grand-unified picture.

2. The structure of NGC 4151

Our model for the nucleus of NGC 4151 (Cassidy & Raine 1996) is sketched in Fig. 1 and the main parameters listed in Table 1. There are three emission line regions: the broad (BLR), intermediate (ILR) and narrow (NLR) line regions. The BLR consists of clouds injected from the surface of an externally heated accretion disc (as a result of Kelvin-Helmholtz instabilities) into a supersonic radial outflow, where they are accelerated and destroyed by ram pressure. The parameters of the system (the luminosity of the central ionising source, L_r , the black hole mass, M_{bh} , and the momentum flux in the wind, L_m) determine the inner and outer radii of the BLR, r_{in} and r_{out} , the flaring of

Table 1. Table of model parameters

Symbol	Quantity	Value in NGC 4151
L_r	bolometric luminosity	$3 - 40 \times 10^{43} \text{ erg s}^{-1}$
L_E	Eddington limit luminosity	$4 \times 10^{45} \text{ erg s}^{-1}$
M_{bh}	black hole mass	$3 \times 10^7 M_\odot$
L_m	momentum flux in wind	$\leq 5 L_E$
r_{in}	inner radius of BLR	$1.4 \times 10^{16} \text{ cm}$
r_{out}	outer radius of BLR	10^{17} cm
v_n	cloud injection speed normal to the disc	$2 \times 10^8 \text{ cm s}^{-1}$
v_ϕ	azimuthal cloud velocity	
$v_{\phi 0}$	initial value of v_ϕ	$6.3 \times 10^8 r_{16}^{-y/2} \text{ cm s}^{-1}$
t_s	sound crossing time in cloud at formation	$5 \times 10^3 r_{16}^2 \text{ s}$
t_c	cloud survival time	$2t_s$
A_d	disc albedo	0.3
n	cloud density	$3.6 \times 10^{12} r_{16}^{-2} \text{ cm}^{-3}$
N_c	column density in clouds	$10^{23} / (1 + (t/t_s)^2) \text{ cm}^{-2}$

the disc in the BLR region and the cloud density and column density. The injection velocity of the clouds at the disc surface, \mathbf{v}_{in} , has a normal component v_n of the order of the sound speed at the Compton temperature of the radiation field falling on the disc; the azimuthal component is taken to be the Kepler velocity at the injection radius. Part of the observed line emission comes from radiation reflected from the disc surface. The disc is opaque in the BLR and therefore obscures clouds on the far side. Assuming a value for the albedo of the disc, A_d , enables the line profiles from the cloud emission to be computed as a function of viewing angle for a specified ionising continuum. The three components of the cloud velocities are computed assuming the cloud dynamics is governed by gravity and ram pressure acceleration and that a cloud loses most (90%) of its mass through the flanks over a time, t_c , of the order of the sound crossing time, t_s in the cloud at formation. For definiteness, we fix this as $t_c = 2t_s$. The sound crossing time is short compared with the crossing time of the BLR at the cloud speed, so the BLR geometry is disc-like. The reflected component of the line emission is Doppler shifted by the rotation of the disc, which is taken to be Keplerian.

The luminosity of the source is estimated from observation and the parameters M_{bh} , L_m , v_n and A_d and the viewing angle are chosen to fit the profile of the CIV $\lambda 1459$ line when the nucleus is in its high luminosity state (Fahey et al. 1991). These parameters appear to be fairly well constrained by fitting the CIV line profile alone given the cloud survival time. The density in the innermost clouds, $n \sim 10^{12} \text{ cm}^{-3}$ gives an ionisation parameter for $r_{in} = 10^{16} \text{ cm}$ consistent with the line ratios, this small BLR size being confirmed by the line variability over 8-16 days in CIV and Ly α (Clavel et al. 1991) and over 9 ± 2 days in H β (Maoz et al. 1991). The BLR is stratified ($n \propto 1/r^2$) and the run of density is consistent with a relatively weak CIII] $\lambda 1909$ line. For a Mathews and Ferland (1987) spectrum we find general agreement for the usual diagnostic line ratios (see Table 2 in Cassidy & Raine, 1993). We find $M_{bh} = 3 \times 10^7 M_\odot$,

$r_{in} = 1.4 \times 10^{16} \text{ cm}$ and $r_{out} = 10^{17} \text{ cm}$, $v_n = 2 \times 10^8 \text{ cm s}^{-1}$; also, $L_m/L_E \leq 5$, where L_E is the Eddington limit luminosity, and $A_d = 0.3$. Under the combined effects of surface heating by the external radiation and the action of the ram pressure of the nuclear wind, the disc flares to an angle of about 30° as required to fit the kurtosis (width at half maximum/width at zero intensity) of the CIV line. The angle of the line of sight to the disc is then 32° . For fixed values of the other parameters this angle is constrained to within at most a few degrees by fitting the profile of CIV by eye. (This is because line profile changes are quite marked as the line of sight approaches the angle of the flared disc.) The presence of line emitting material close to the line of sight to the continuum source is consistent with the observed response of the lines to changes in the ionising continuum with a delay of less than 3 days (Clavel et al. 1991) and this is confirmed by the non-zero response at zero continuum lag in the 1D transfer function (i.e. the line response to a δ -function ionising continuum (Blandford & McKee 1982)). Details of the transfer functions obtained by Horne & Ulrich (1996) can also be accounted for (see Sect. 5.1). Further details are given in Cassidy & Raine (1996).

As it declines in luminosity NGC 4151 changes its classification from a Seyfert 1 to close to a Seyfert 2. In this transition the shapes of the emission and absorption lines change, so this is not just an effect of the loss of ionising photons. The lifetime of the BLR clouds is $10^4 r_{16}^2 \text{ s}$, so rapid changes in structure are possible. From the low state profiles we deduce the existence of the ILR lying in the range $3 \times 10^{17} \text{ cm} < r < 10^{19} \text{ cm}$. (See also Brotherton et al. 1994.)

We have suggested (Cassidy & Raine 1996) that the ILR arises from a thermally driven disc wind (compare Smith & Raine 1985), hence that it too has a flattened geometry. We have shown also that, in the low state, the inner BLR clouds disappear, enabling us to explain the changes in the CIV profile width and equivalent width. Other optical and UV line ratios and profile characteristics in the various luminosity states can also be accounted for.

2.1. Debris from the BLR clouds

The warm material from the dispersing BLR clouds forms a scattering medium. The optical depth can be estimated as follows. Let the clouds rise from the disc over an area A and let the mass input into the clouds be \dot{M} . Suppose the heating timescale for the cloud debris is t_h . The column of warm dispersing material is

$$N_h \sim \dot{M} t_h / m_H A.$$

We have $t_h = kT/\Gamma$, where $\Gamma = (\sigma_T/m_e c^2)(L/4\pi r^2)4kT_c$ is the Compton heating rate for a Compton temperature T_c . This gives $t_h \sim 10^8 r_{17}^2 (L/L_E) m_8 \text{ s}$ at $10^{17} r_{17} \text{ cm}$. We estimate the mass flow rate into the BLR of NGC 4151 by comparing the model line flux for CIV $\lambda 1459$ with the observed flux in the high luminosity state. For a distance to NGC 4151 of 20 Mpc we obtain a mass flux of $2.4 M_\odot \text{ yr}^{-1}$. Then, with $d\dot{M}/dr \propto 1/r$,

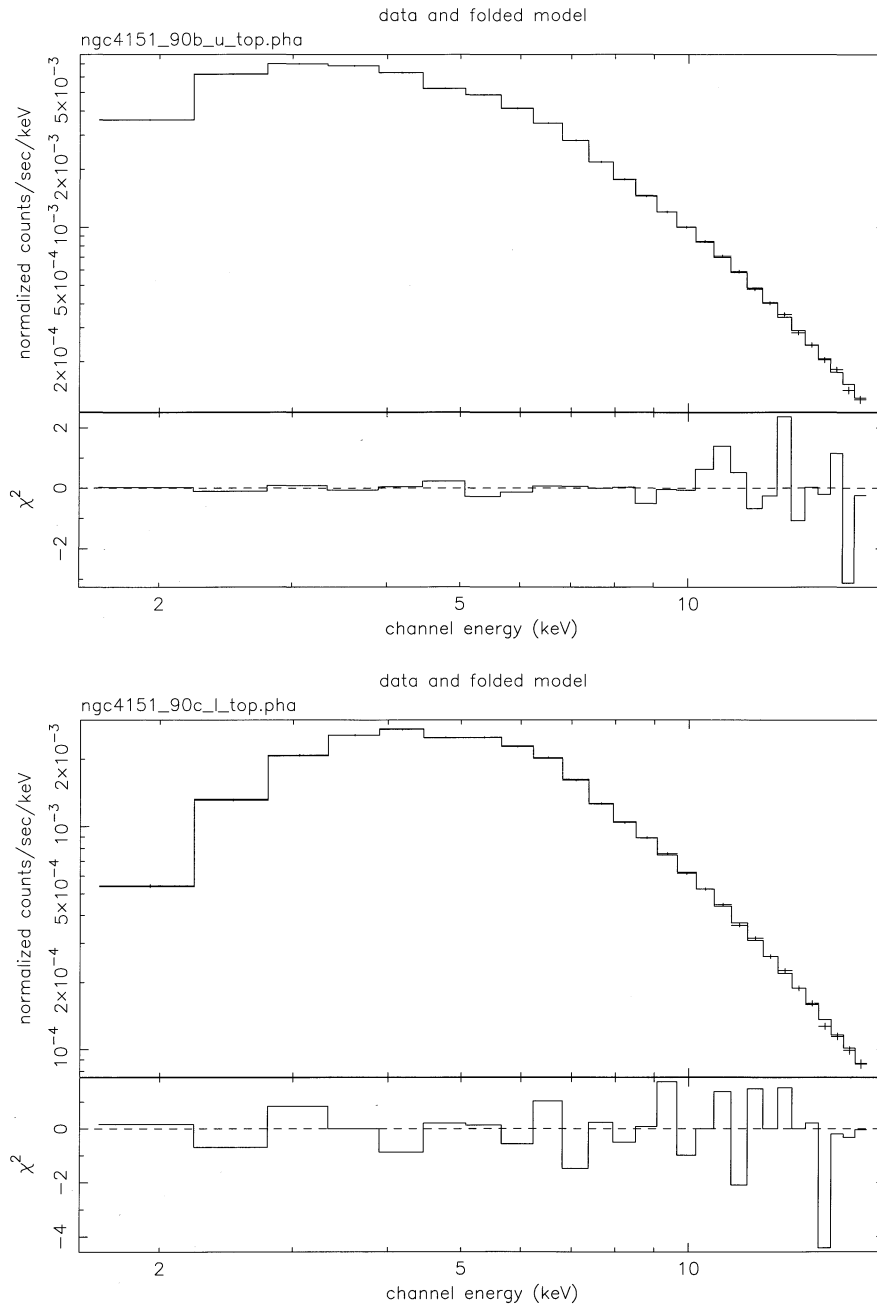


Fig. 2a and b. X-ray counts and folded model and χ^2 versus energy for Ginga observations of NGC 4151 for **a** May 1990 and **b** Nov 1990.

we find that the dispersing column has an electron scattering optical depth of $0.1(L/L_E)m_8$.

The cloud velocity on break-up is much less than the wind velocity, v_w . The acceleration timescale for the dispersing material of thickness h , density n_c and temperature T_c to reach the ambient wind velocity is $(n_c/n_w)(h/v_w)$. Taking for $n_c h$ an upper limit for the column density of 10^{23}cm^{-2} , as in the clouds, and putting $n_w = 4 \times 10^6 (L_m/L_E) r_{16}^{-2} \text{cm}^{-3}$ from Cassidy & Raine (1996) gives an acceleration timescale $\leq 2 \times 10^8 (10^4 \text{K}/T_c) r_{17}^2 \text{s}$, of order of the heating timescale. Thus, once the material has started heating it is rapidly dispersed. In other words, most of the debris is in material heating to 10^5K and moving with the clouds. It will therefore contribute

a scattered broad-line component that is polarised transverse to the disc axis and which is not significantly broader than the unscattered flux. Note that the scattering into the line of sight that has been observed from much more extended regions (Sect. 5.3), and probably dominates in NGC 1068, must have a different explanation (Capetti et al. 1995; Antonucci et al. 1994).

2.2. X-ray properties

The variability of the X-ray source in NGC 4151 means it must lie within 10^{15}cm ; the nuclear wind is optically thin to electron scattering to this radius.

The dispersing material from the inner clouds provide warm absorbing material in the line of sight to the X-ray continuum source and the outer BLR clouds partially cover the source. The model suggests therefore that in this object we have a *combination* of warm absorber and partial coverer for the X-rays when the nucleus is in its high luminosity state. Reynolds & Fabian (1995), in discussing MCG 6-30-15, have also pointed to the possibility that the dispersing BLR material may provide the X-ray warm absorber. Yaqoob & Warwick (1991) excluded a warm absorber in their analysis, but Warwick et al. (1995) find that a modest level of ionisation provides the required decrease in opacity in the 1-4 keV band whilst maintaining an iron K-edge energy consistent with the average of ~ 7.3 keV derived in the Ginga observation (Yaqoob et al. 1993). Weaver et al. (1994a & b) model the ASCA data with either a dual cold absorber plus soft excess components, or a warm absorber plus a scattered continuum.

It follows that limited data can not be used to distinguish between models. Nevertheless it is of interest to note that it is possible to fit the very different Ginga spectra (using XSPEC) of Nov 1990 and May 1990 (Yaqoob et al. 1993) within the context of our model. We use a power law continuum with a photon index Γ plus low energy absorption due to a uniform column ($N_H = 10^{22} \text{ cm}^{-2}$) of cold gas. This column could represent the ILR or, possibly, the outer disc material in the line of sight. The abundances used are solar, except iron which is fixed at twice solar. An iron emission line and edge are also included. The iron K-edge and emission line energies are fixed at 7.1 and 6.4 keV respectively. (Allowing them to vary does not improve the fit.) The iron line is narrow in both fits ($\sigma = .1$ and equivalent width approximately 22eV), but is not very well constrained by the data. The column density varied from $2 \times 10^{23} \text{ cm}^{-2}$ in May 1990 to $7.4 \times 10^{22} \text{ cm}^{-2}$ in Nov. 1990, while the covering factor varied from .16 to .57. In the former case we found $\Gamma = 1.76$ and in the latter $\Gamma = 1.61$. The respective reduced χ^2 values are .71 and 1.12 for 35 df (Fig. 2). In the earlier observation the warm absorber dominates and in the latter the partial coverer. Yaqoob et al. (1993) fit their data with a partial coverer only, but with an iron abundance that is required to vary between data sets by a factor of 5. With the inclusion of the warm absorber component we find the iron abundance can be held constant.

Yaqoob et al. also claim that the dip in the covering factor and the increase in column density *rule out a cloud model* for the absorption and suggest a ‘bulk’ structure the geometry of which is at least most of the time stationary relative to the X-ray source. In their view the edge of an accretion disc or a torus is an obvious candidate. An explanation in the context of our model could be that an increased radiation pressure or ram pressure in the wind is flattening the cloud trajectories giving rise to an increase in column and a decrease in covering factor of the X-ray source. Our conclusion is therefore that our model is *not* ruled out by current X-ray observations.

The small angle of the line of sight to the disc is consistent with a very weak reflected hard X-ray component (Maisack & Yaqoob 1991) in contrast to Pedlar et al (1992) who suggested an angle of about 40° to the radio axis.

2.3. UV Features

We expect UV absorption lines to arise in the outer BLR and ILR clouds from the covering of both the UV continuum source and the inner line emitting clouds. The absorption lines are narrow because the flaring of the disc means that the outer clouds are moving across the line of sight when they cross the inner clouds (compare BAL QSOs below). The absorption will be complex and comparison with observation will have to await detailed modelling. Bromage et al. (1985) argued that a column of $40 - 180 \times 10^{21} \text{ cm}^{-2}$ of gas at $10^4 - 10^5 \text{ K}$ could be responsible for both the UV and soft X-ray absorption which would be consistent with our proposal. On the other hand while Ulrich (1988), locates the absorbers at $\sim 10^{17} \text{ cm}$ with a density in the range $10^{8.5} - 10^{10} \text{ cm}^{-3}$, consistent with our outer BLR clouds, she finds an EW of the CIV absorption of $4 - 10 \text{ \AA}$. This translates to an equivalent H-column of 10^{19} cm^{-2} if all carbon is ionised to C^{+++} and the lines are optically thin, and implies that the UV absorption is occurring in a separate component. The final assumptions may however be incorrect: a photoionisation calculation using the CLOUDY photoionisation code shows that there is substantial C^{++} in our optically thick outer BLR clouds. Thus it remains to be seen whether the outer BLR clouds are responsible for the UV absorption.

The disc, broad-line clouds and the cloud debris will absorb ionising radiation from the central source outside of a cone centred on the disc axis. To obtain the angle of this cone requires detailed modelling since we need to estimate timescales to better than a factor 2. The following estimate shows only that the obscuration by the debris in the UV could be consistent with the observed emission cone. The cloud material rises above the disc through an angle $\tan^{-1} v_i(t_c + t_a)/R_{BLR}$, where t_a is the acceleration timescale over which the trajectories of the debris in the wind become effectively radial. Estimating the timescales as above gives $t_c = N_{col}/(n_c c_s) \sim 10^7 \text{ s}$ at 10^{17} cm , for a column of 10^{23} cm^{-2} and a gas density in the clouds of $3 \times 10^{10} r_{17}^{-2} \text{ cm}^{-3}$, and $t_a \sim 2.5 \times 10^8 r_{17}^2 \text{ s}$. Thus, $t_a \gg t_c$ and we can neglect the motion of the undisrupted cloud. The disc rises to an angle of 30° , a height of $6 \times 10^{16} \text{ cm}$ at 10^{17} cm . So the debris, at its input velocity of $2 \times 10^8 \text{ cm s}^{-1}$, rises to about $\tan^{-1} 1.1$ or about 50° . Thus, the unobscured ionising cone has a full angle of about 80° . Within this cone ionising flux escapes to the NLR. Evans et al. (1993) give $75 \pm 10^\circ$ for the full cone angle. The radio jet is presumably associated with collimation of the nuclear outflow along the axis (Smith & Raine 1985).

3. Intermediate Seyferts and True Seyfert 2s

For the purpose of matching profile changes in a single galaxy the disappearance of the inner BLR clouds can be attributed either to obscuration or to the suppression of cloud formation. These two alternatives will give very different predictions for different lines of sight if the obscuration is angle dependent. Changes in ionisation parameter have also been proposed (Kwan 1984). However, Kwan considered only changes in line ratios; the line *profile* changes observed in NGC 4151 cannot be

explained in our picture by variations in ionisation parameter alone. We shall now argue that observational evidence supports the case that the formation of the inner clouds is indeed suppressed in variable objects in their low luminosity states. Some of the distinctive predictions of our unified picture follow from this conclusion.

Variability observations of some AGN seem to support the hypothesis that changes in classification can be explained by dust clouds crossing the line of sight. For example, Fairall 9 ($M_V = -24$), a quasar with a Seyfert 1 spectrum at the time of discovery (Ward et al. 1978) was by 1984 a Seyfert galaxy ($M_V = -21$) with a spectrum approaching that of a Seyfert type 2 (Kollatschny & Fricke 1985). Most of the change appeared in the years between 1981 and 1984.

However, a number of Seyfert galaxies are known to change their classification along the sequence between type 1 and type 2 on timescales of weeks to months (Antonucci & Cohen 1983; Ulrich et al. 1984; Wamsteker et al. 1985; Andrillat & Souffrin 1968), which makes it unlikely that a dust cloud in a torus moving across the line of sight is responsible. The broad $H\beta$ line in NGC 5548 disappeared in less than three months during 1992, when the nucleus changed from the usual Seyfert type 1.5 to a type 1.9 (Jijima et al. 1992; Penfold 1992, 1992a).

Loska et al. (1993) modelled a dust cloud surrounding the nucleus of NGC 5548, and found that a drop in the luminosity by a factor of 5 can result in the appearance of dust grains at distances as small as 4 lt-weeks but the time-scale of formation of these new dust grains is far too long to explain the changes. In addition, it is difficult to explain why the disappearance of the lines is not accompanied by a corresponding fall in the continuum luminosity if the line weakening is due only to the increased dust extinction. They conclude that the observed changes are independent of the presence of dust.

Similar observations to the ones in NGC 5548 were made by Alloin et al. (1985) when monitoring the nuclear $H\beta$ and $H\alpha$ emission profiles of the Seyfert galaxy NGC 1566. The spectrum changed from one closely resembling a Seyfert type 1.9 to one resembling a Seyfert type 1.2, with most of the changes taking place within 4 months. The nonstellar continuum component increased by a factor of 5 at 3700 Å over this period. The Balmer decrement in both broad and narrow components is low in NGC 1566, implying little or no dust across the BLR and NLR. The $H\beta/H\alpha$ ratio was, within the uncertainties, constant in time.

If dust extinction were the cause of the disappearance of the broad emission lines, the fading of the continuum and the disappearance of the broad emission lines would be simultaneous events. However, Penston & Perez (1984) observed that the decrease in emission line widths in NGC 4151 and 3C 390.3 followed the fading of the continuum. Furthermore, Inda et al. (1993) argue that the X-ray variability in 3C 390.3 is unlikely to be caused by changes in the nuclear obscuration by cold matter because the tenfold intensity reduction observed by EXOSAT was not accompanied by marked changes in the spectrum (eg. a deep Fe K-edge).

Also, if the difference between Seyfert 1s and Seyfert 2s were the result of angle dependent dust extinction, then one would expect a continuous change in the continuum and emission properties from Seyfert 1s through the intermediate Seyferts to Seyfert 2s contrary to what is observed. Ulvestad (1986) studied 11 Seyfert 1.8 and 1.9 galaxies as well as Seyfert 1.2 and 1.5 galaxies. He found that the ratio of radio to featureless optical continuum luminosity in type 1.2, 1.5, 1.8 and 1.9 galaxies lies between the low value found for Seyfert 1s and the much higher radio/optical ratio for Seyfert 2s. However, there is no significant difference in this ratio between the type 1.2/1.5 nuclei and the type 1.8/1.9 nuclei. He further claims that it is unlikely that this trend is caused by increasing dust obscuration of the optical continua along the sequence from Seyfert 1 through to Seyfert 2 galaxies because the featureless optical continua of the intermediate Seyferts and type 2 Seyfert galaxies do not appear to be highly reddened.

These observations indicate that profile changes must be caused by intrinsic modifications in the source. This in turn implies that the BLR is very close to the nucleus and that the emission line region that contributes most to the profile is not large in extent. *Our model BLR of NGC 4151 fits these criteria exactly.* The changes can be explained by the suppression of cloud formation at low luminosity which we predict. For a cloud density of $3 \times 10^{12} r_{16}^{-2} \text{ cm}^{-3}$ and constant cloud column of 10^{23} cm^{-2} the BLR cloud lifetime is shorter than the light travel time for $r < 10^{17} \text{ cm}$. Thus the light travel time determines the transition timescale for intermediate Seyferts. Temporary changes in the classification of NGC 5548 and NGC 1566 can also be explained by the destruction (or non-creation) of broad-line clouds. A test would be to look for a reduction in the scattered polarised flux in the broad lines at low luminosity.

Note that we should distinguish here between the suppression of cloud formation in our model of NGC 4151 in its low luminosity state, which is a consequence of the substantial variability of the source, and a general suppression of cloud formation in low luminosity systems, which in our model occurs only for the ILR clouds. Thus, according to the model, large variations in accretion rate could suppress cloud formation for up to the mass inflow timescale from the BLR, but at steady low luminosities the BLR clouds should always be present. As a consequence we predict the existence of true Seyfert 2 types in variable systems.

Support for the ‘missing BLR’ scenario comes from the observed typical lack of polarisation in the featureless continua of some Seyfert 2 galaxies, because if a hidden region were to produce the continuum, it could only be observed by scattering, and should therefore be significantly polarised. The detection of narrow line radio-loud or radio-quiet objects which do not show a large column density in their X-ray absorption and possessing a variable, unpolarised continuum should settle this point.

At present there is observational evidence for few such objects. Kay (1994) carried out a near UV spectropolarimetry survey of 50 Seyfert 2 galaxies and failed to detect in most objects a significant amount of polarisation in the featureless continuum. Only a few objects in her sample could possibly possess a hidden

BLR. Tran (1995) also points out the possibility that there ‘exist the genuinely pure’ Seyfert 2 galaxies that do not contain BLRs and the appearance of which is independent of the observer’s line of sight.

NGC 5506 is generally considered to be a bright Seyfert 2 galaxy and is a possible candidate for a true Seyfert 2. Since the source is variable, a weak BLR may be present at some epochs, so this classification is compatible with detection of, for example, weak broad $H\alpha$ in isolated observations (Shuder 1980). Broad Paschen β (1500 km s^{-1} FWHM) was observed by Blanco et al (1990). Since the X-ray luminosity is high and activity is significant on a timescale of about 10^3 seconds (McHardy & Czerny 1987) the X-ray emitting region is unlikely to be covered by a thick dusty torus and one can reasonably assume that this region is observed directly as in Seyfert 1 galaxies. Pounds et al (1989) show that the spectrum may be fitted with an iron fluorescence line at 6.4 keV and an iron K absorption edge at 8.3 keV. This has been taken to indicate ionised gas in the line of sight. Also, if the large dip that appears between ~ 8 and 12 keV is due to Fe K-shell absorption, then it corresponds to a large column density of $(0.7 - 1.9) \times 10^{23} \text{ cm}^{-2}$ as in other Seyfert 2s. However, good fits were obtained without an ionised absorber from enhanced reflection ($1.5\times$), corresponding to a ‘saucer-shaped’ disc, and a $2\times$ solar iron abundance. The underlying power-law slope in the reflection model is 0.9. Smith and Done (1995) also prefer a face-on disc for NGC 5506 and associate the observed absorption with the line-of-sight column through the host galaxy rather than a molecular torus.

Pogge (1989) found that maps of the $[\text{OIII}]\lambda 5007 / (H\alpha + [\text{NII}])$ emission ratio, which emphasises regions of high ionisation gas, reveal distinctly conical high-ionisation regions, with the nucleus at the apex in four Seyfert 2 galaxies. Three out of nine Seyfert 1 galaxies showed evidence for spatially extended ionised gas regions, compared with 8 out of 11 Seyfert 2s. Pogge argues that these results are inconsistent with the SPM. Six Seyfert 1s and 3 Seyfert 2s are compact, with no suggestion of marginally resolved nuclear substructure. These compact Seyfert 2s are at least consistent with the conclusion that not all Seyfert 2s are viewed edge-on and consequently that the BLR may be temporarily absent in some Seyfert 2s, not just obscured.

One of the difficulties associated with finding true narrow line objects is the uncertainty whether the absence of broad-lines is caused by the absence of electron scatterers or by the absence of broad-line clouds. In our model, of course, the absence of scatterers arises from the absence of clouds, so a Seyfert without broad lines in its polarised spectrum must be a true Seyfert 2.

The conical geometry of the NLR in NGC 4151 clearly indicates anisotropy probably due to some obscuring material. If our model of NGC 4151 is to be extended to all Seyferts there must also be a torus of material that obscures the direct view of the nucleus at low latitudes. We turn to this in the next section.

4. Obscured Seyfert 1s and dusty molecular Tori

NGC 4151 is an unobscured Seyfert 1 galaxy. According to the SPM unification it must therefore be observed along the opening cone of the torus, that is within 30° of face-on. Yet Merlin/VLA radio studies of NGC 4151 show that collimated ejection is taking place along PA $\sim 77^\circ$ and 257° giving rise to a two-sided radio jet. Also, the X-ray column in our line of sight to NGC 4151 is large and most of the X-ray source is quite obscured from our point of view. These X-ray and radio properties are more suggestive of an edge-on Seyfert than a face-on one.

If we are to include NGC 4151 in a unification scheme therefore, we must adjust the parameters of the obscuring material. We begin by presenting some further evidence in favour of such adjustments by showing that a dusty molecular torus with small fixed opening angle cannot be a universal feature of AGN, even excepting NGC 4151.

(i) X-rays: Lawrence (1991) has argued that much of the X-ray absorbing material in AGN is free of dust, and that narrow-lined and reddened broad-lined objects occur more frequently at lower source powers. There must be a large range of geometrical thicknesses and optical depths in the absorbing material. He speculates that the obscuring material is not a molecular torus but an expelled shell of gas. A luminosity dependent flaring of the obscuring disc could also explain why the fraction of narrow-lined AGN is a decreasing function of source power. Reichert et al. (1985) find that when comparing the X-ray column densities with optical reddening indicators little, if any, dust can be associated with the X-ray absorbing regions. Mulchaey et al. (1992) attribute the observed range in column densities in a sample of Seyfert 2s to intrinsic variations in the thickness of the obscuring medium and a variation of the angle to the line of sight. They also state that if all Seyferts have a 30° opening angle, as required by the standard model, and if all tori are transparent to hard X-rays, then the Seyfert 2s would overproduce the hard X-ray background. A 30° angle also conflicts with the observed low polarisation of the featureless continuum, which suggests a larger opening angle (Antonucci 1993).

(ii) Radio galaxies: A range of torus opening angles (at the very least) also seems to be indicated for FR II type radio galaxies and quasars (Heckman et al. 1986; Hutchings 1987).

(iii) Multi-band spectra: The lack of diversity in the shape of the optical-ultraviolet continuum of Seyfert 1 galaxies, radio-quiet and radio-loud quasars argues against large amounts of dust extinction (Neugebauer et al. 1984, 1986), since the effect on the continuum slope is likely to be large, even for a small amount of dust. Baker & Hunstead (1995) have presented low resolution, composite optical spectra for 60 (radio-loud) quasars. They found that with increasing inferred viewing angle to the radio-jet axis, the optical continuum steepens, the 3000\AA broad emission feature decreases in relative strength, and the narrow-line equivalent widths and Balmer decrement increase. They also found that reddening is considerable ($A_v \sim 2.4$) in most lobe-

dominated quasars. A significant amount of dust must therefore lie within the opening angle of the torus and there may be no well-defined opening angle at all. If radio-quiet quasars (QSOs) possess as much dust as the radio-loud ones and have gone undetected at other wavelengths then up to 80% of radio-quiet quasars could be obscured by dust up to $A_B = 5$ mag. (Webster et al. 1995). This would be difficult to reconcile with our model. However, Boyle & di Matleo (1995) use a sample of X-ray selected QSOs to place a limit on the intrinsic amount of dust of $A_B < 2$ mag. They also observe a similar spread in the X-ray-to-optical flux ratios in an optically selected sample of QSOs. Their interpretation is that most of the scatter is probably due to effects other than dust obscuration. Hence, it seems unlikely that a significant population of highly obscured QSOs exist in X-ray selected samples. These studies can be reconciled if radio-loud quasars have systematically much larger amounts of associated dust than radio-quiet QSOs.

The same argument applies to the continua of Seyfert 2 nuclei. Their non-stellar optical, ultraviolet and X-ray continua are very weak, but their ratios are not too different from those in Seyfert 1s. Therefore, the overall continuum shape is similar in both groups. There is also no evidence for dust as a major constituent in terms of severe modification of the intrinsic spectrum in blazars (Sanders et al. 1989).

(iv) Infrared: However the near IR distribution in most AGN show features that can be attributed to hot dust emission: a minimum at about $1 \mu\text{m}$ (Sanders et al. 1989) and a bump peaking at $3\text{-}5 \mu\text{m}$ (Edelson & Malkan 1986; Robson et al. 1986). According to Giuricin et al. (1995) the lack of a good correlation between the near and mid IR on the one hand and the $100\mu\text{m}$ emission on the other is interpreted to mean that the bulk of the FIR band comes from the host galaxy while the NIR and MIR is nuclear. NGC 1068 is considered to be exceptional in a number of ways. The far infrared is resolved and originates from a 3 kpc diameter star formation ring (Telesco et al 1984; see also Rodriguez Espinosa et al. 1986, 1987; Clement et al 1988 for similar conclusions in other systems). The X-ray column is high, $> 10^{24} \text{ cm}^{-2}$ (Mulchaey et al. 1992) possibly as a consequence of the edge-on view through the obscuring ring. The origin of the mid-infrared is still being debated, but is generally thought to be associated with dust emission in both radio loud systems (Heckman et al. 1992, 1994; Efstathiou & Rowan-Robinson 1995) and Seyfert galaxies (Giuricin et al. 1995; Maiolino et al. 1995, Heckman et al. 1995). Some variability timescales are also in agreement with dust emission (Bregman 1991).

How can we extend our picture of NGC 4151 to be compatible with this evidence? Viewed from close to the plane of the disc the line of sight to the BLR and ILR passes through the flared disc. The optical depth through the disc is determined by the density at the inner edge. The density of hot material near the disc surface is of order $6 \times 10^8 r_{16}^{-2} \text{ cm}^{-3}$, ignoring parameters of order unity (Cassidy & Raine 1996). If the obscuring disc consists of a hot isothermal externally -heated atmosphere above a standard α -disc the density falls off along a

line of sight through the atmosphere as $r^{-15/8} e^{-\text{const}/r}$, which is steeper than $1/r$.

The column to the inner BLR at 10^{16} cm is then no more than $\sim 6 \times 10^{24} \text{ cm}^{-2}$. This would be sufficient to account for the reduction in hard X-ray flux by electron scattering out of the line of sight in the majority of obscured systems. However, it is clear that in order that it be completely suppressed, the direct soft X-ray emission requires photoelectric absorption, hence cooler gas. In addition, the broad-line emission is completely blocked from direct view by 10 - 100 magnitudes of extinction. It is therefore impossible to contrive a model that does not involve dust. The above calculation shows with the normal gas/dust ratio there would be sufficient material in the line of sight in the disc to produce the required extinction (a column of $6 \times 10^{24} \text{ cm}^{-2}$ corresponds to an A_v of 500), but in the externally illuminated disc atmosphere it is too hot for the dust to survive. The simple picture of a dusty, but otherwise standard, accretion disc extending inwards into the BLR region is untenable. Nevertheless we have in NGC 4151 direct evidence for the presence of dust not in the line of sight through observations of Si and forbidden Fe emission lines in the infrared (Thompson 1995). Thus, we may assume that there is some cold dusty material that would be in the line of sight at low inclinations only. This material must be between the BLR and NLR, beyond the region of disc flaring associated with the BLR (so could be in the ILR region). The response of this material to its environment will be important when we consider highly luminous Seyferts and quasars and is discussed in Sect. 6.

5. An alien view of NGC 4151

We can now consider how the model of NGC 4151 would appear viewed first from angles more face on to the disc, and then from closer to the disc plane. We shall argue that this is the basic structure of all AGN. Referring to Fig. 1 we see at edge-on angles to the line of sight the direct view to the nucleus is blocked. Such a system would be classified as a Seyfert 2 with scattering into the line of sight giving polarised broad-line component and a weak X-ray continuum. At larger angles to the disc the line of sight passes through the BLR clouds giving objects such as NGC 4151 and NGC 3516. At somewhat larger inclinations the X-ray source is covered by the warm absorber only: an example is NGC 5548. Face on objects have no absorption and relatively narrow lines.

5.1. Line profiles and transfer functions

The BLR is usually assumed to be a spherical distribution of clouds. To obtain a sufficiently narrow transfer function for the response of the broad lines to changes in the ionising continuum in NGC 5548 Ferland et al. (1992) has proposed that anisotropic emission from the clouds must be considered. In NGC 4151 the transfer function is narrow (Netzer 1990) but, in contrast to NGC 5548 the response is immediate. To match this behaviour it would be necessary to assume the emission from clouds in NGC 4151 is not anisotropic. Indeed, with anisotropic emission

it would be difficult to see how the MgII and CIV profiles in NGC 4151 could be similar (except in the extreme wings). An alternative possibility is to assume a flattened cloud distribution for *both* cases. This gives a narrow transfer function for short continuum pulses, but different delays for different lines of sight. This can be seen by comparing the non-zero delay from a face-on disc with the immediate response from a sphere of the same radius. A narrow width and immediate response are confirmed by numerical computation for the case of NGC 4151 (Cassidy & Raine 1996). Note also that we obtain different lags for different continuum pulse lengths which again is a consequence of a non-spherical geometry. For an edge-on line of sight a flattened configuration exhibits an immediate line response to continuum changes. More face on systems show only a delayed response as in NGC 5548 (Ferland et al 1992). In Fig. 3 we show a comparison of the transfer functions for a model system with an inner disc radius of 4×10^{16} cm and a disc inclined at 24° to the line of sight with one at 75° . At the higher inclination (75°) the lag of the initial line response to the continuum is about one week, but note that the peak in this case comes earlier than that for lower inclination.

Both Done & Krolik (1996) (for NGC 5548) and Ulrich & Horne (1996) (for NGC 4151) find some evidence that the peak of the transfer function for the red wing comes earlier than that for the blue wing of the line. The existence of a reflected component to the lines (as a result of reflection in the disc) explains the different responses of the red and blue wings with that for the red wing being more disc-like (narrow and sharply peaked). The transfer function for the blue wing is broader. These results arise from the non-spherical cloud distribution. For a spherical geometry, a contrived velocity field is required to obtain this behaviour (eg Mathews 1993).

Note that although the line profile widths decrease for more face-on discs, they do not become exceptionally narrow when viewed face-on because the clouds have a velocity component normal to the flared disc. In fact, the narrowest lines occur for a disc at $\sim 75^\circ$ as a result of flaring. We note that, if the disc surface is smooth, the reflected component will tend to be polarised in the plane of the disc. However, by construction, the disc surface in the BLR is far from smooth and this will tend to de-polarise the reflected component.

5.2. Predictions for X-ray absorption

In Sect. 2.2 we considered the X-ray properties of the model specific to NGC 4151. We now extend the discussion to different lines of sight. Over a range of angles, the line of sight to the X-ray source will intersect the outer region of the disc and the broad-line clouds. At larger angles, it will pass through the ILR clouds and the warm debris from clouds as they are disrupted and heated to the Compton temperature. We would expect these systems to exhibit complex X-ray absorption. A few systems like NGC 4151 should contain the cold outer screen of one or both of the flared disc and ILR clouds, either totally or partially covering the central X-ray source. In these systems there will be a combination of partial covering by the BLR clouds,

which should vary with the BLR lines, and by a warm absorber. At larger angles to the disc this complex system should be replaced by a warm absorber or, possibly, a combination of warm absorber and ILR. Since the BLR is directly visible, these will be nuclei of intermediate Seyfert type (NGC 5548 is a typical example) or, at higher luminosity, Seyfert 1s. Note that the cloud debris exists over a range of temperature so detailed modelling is required to confirm that this material can be both the source of the electron scatterers (which requires a temperature approximately 3×10^5 K) (Antonucci, 1993) and the warm absorber (which needs $T \geq 10^5$ K (Pounds et al. 1990)).

To compare these predictions with observations we note the following points. The X-ray continuum in radio-quiet systems is usually fitted by an underlying power-law with an average photon number index of 1.8 - 1.9 once a number of features have been removed. These features include an iron emission line near 6.4 keV, a ‘hump’ above ~ 10 keV and in some Seyferts a ‘warm’ iron K-absorption edge (Nandra & Pounds 1994).

The K-absorption edge at 8-9 keV indicates a substantial column density of highly ionised matter, a so-called ‘warm absorber’, in the line of sight to several AGN, including some with otherwise ‘bare’ Seyfert 1 nuclei (Pounds et al. 1990; Smith & Done 1995). This warm absorber can also account for the spectral variability and soft excess evident in Ginga and some EXOSAT data. The warm absorber can change rapidly only if its density is high, $\geq 10^7$ cm $^{-3}$ (Pounds et al. 1990).

Nandra and Pounds (1994) find that their lowest luminosity warm absorber (NGC 4051) is at a maximum distance of $\sim 10^{17}$ cm from the central engine and for the highest luminosity warm absorber (MCG-2-58-22) they obtain an upper limit of $\sim 10^{20}$ cm with a covering factor of the order ≥ 50 per cent. This places the warm absorber at a similar distance from the nucleus as the broad-line region in the disc-wind model. ASCA observations of variable absorption in MCG-6-30-15 have been used to give a (model-dependent) location for the warm absorber in or just beyond the BLR (Reynolds & Fabian 1995). If the warm absorber is not present then the native spectrum will exhibit a large soft excess.

At even higher latitudes we expect to see X-ray absorption associated only with the NLR scatterers (if these exist) and with the galaxy. Such objects will show relatively narrow broad lines. They may also possess an intrinsic *ultra-soft* spectrum particularly if, as is the case in many of the early EXOSAT observations, the power law slope is extrapolated from the hard X-ray band. (And correspondingly the hard tail is missing in such sources.) It is interesting to note that Boller et al. (1996) find narrow line Seyfert 1s have generally steeper soft X-ray slopes with rapid soft X-ray variability and therefore significant electron-scattering of the X-rays seems unlikely in these systems. There is in addition no evidence for large neutral H column densities in excess of the galactic column. Conversely, soft X-ray selected samples of Seyfert 1s contain relatively large numbers of narrower line Seyferts (Stephens 1989; Puchnarewicz et al 1992).

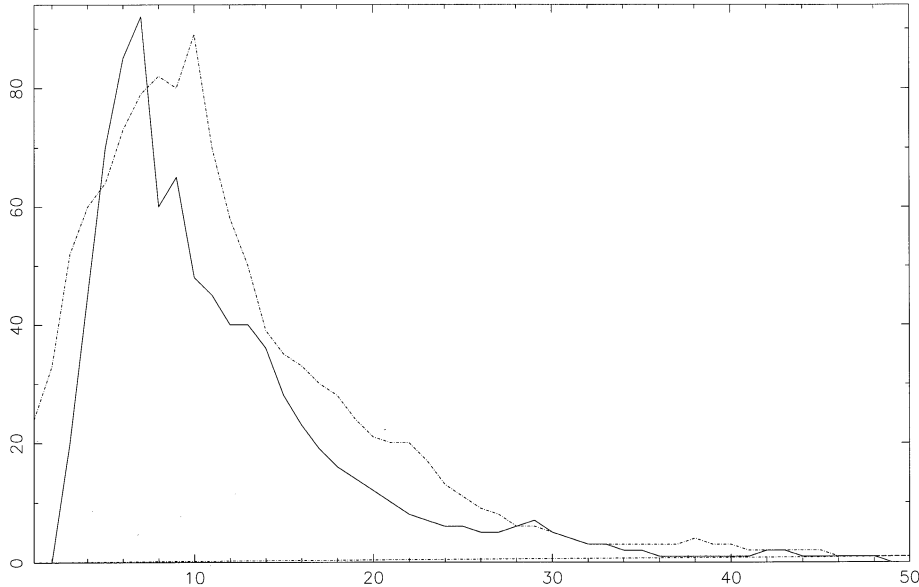


Fig. 3a and b. Transfer functions for the disc-wind model at two disc inclinations **a** (dashed line) 24° and **b** (solid line) 75°

5.3. Scattering into the line of sight

The optical to soft X-ray continuum in Seyfert 2 galaxies is partly radiation scattered into the line of sight. The opening angle of the cone of light incident on the scattering region is deduced to be $\leq 30^\circ$ (Antonucci, 1993) from the fact that the scattered light is polarised perpendicular to the radio jet axis. (The direction of polarisation defines the E-vector prior to scattering.) But this does not require radiation to be *blocked* within a solid cone of this angle; the result can also be achieved if the *scatterers* are associated with a restricted conical shell. In our model the BLR debris provides just such a conical shell. This leaves the opening angle of the obscuring torus as a free parameter. For consistency with our model of NGC 4151 the half angle of the cone unobscured by dust must be at least 60° (since the disc flares to about 30°). Therefore, at the luminosity of NGC 4151, obscured Seyfert 1s make up about half of the observed systems rather than the 80% of the standard model. Since it is in this luminosity range that Seyferts make the most important contribution to the X-ray background this eliminates the problem of overproduction of that background associated with a constant small opening angle (Mulchaey et al. 1992).

Light within the inner unobscured cone escapes to the NLR giving a conical illumination to the NLR clouds (Tadhunter & Tsvetanov 1989; Wilson et al. 1988). There is evidence in NGC 1068 for scattering of this light from material at ~ 100 pc (Antonucci 1993) - as well as scattering from closer in: the multiplicity of the Fe K lines requires the existence of a hot $T \sim 4 \times 10^6$ K component of the scattering medium in addition to the warm $T \sim 2 \times 10^5$ K scattering cloud required by the polarised light. The relative strengths of the Fe K lines indicate that the two components scatter comparable amounts of radiation (within a factor of a few) (Marshall et al. 1993). In their preferred model the warm component extends from 20pc to 100pc while the hot component begins at 1-2 pc.

5.4. The Intermediate Line Region

An intermediate line region (ILR) is essential in our picture of NGC 4151. If this is to be a typical galaxy an ILR must be present in all comparable systems (although it need not be a distinct region: the BLR and ILR may be continuous). There is a growing body of evidence to support this view.

(i) Individual objects:

(a) 3C390.3 is a broad-line radio galaxy exhibiting a Seyfert 1 type spectrum and, like NGC 4151, has appeared close to a Seyfert 2 (really, of course, in this case a NLRG), for example during 1979-80 (Barr et al. 1983). Clavel & Wamsteker (1987) argue that the BLR gas cannot be responsible for the relatively narrow emission lines in the low state, which must come from an intermediate region. Zheng (1996) found that the narrow component (FWHM ~ 2000 km s $^{-1}$ in the Ly α and CIV lines varied by a factor of approximately 2.5 with the CIV/Ly α flux ratio of 0.4, whereas for the broad component this ratio is around unity.

(b) Indications of the existence of an additional emission line region at greater distances than the BLR were also found in 3C382 (Yee & Oke 1981), 3C120 (Oke, Redhead & Sargent 1980), Fairall 9 (Stirpe et al. 1989), 3C 445 (Crenshaw et al. 1988), NGC 7469 (Bonatto et al. 1990), and NGC 5548 (Wamsteker et al. 1990).

(c) Filippenko (1985) investigated Pictor A, a radio galaxy with features of a LINER, PKS 1718-649, a classical LINER, and the QSO MR 2251-1878 and found that in all three nuclei the great strength of [OIII] $\lambda 4363$ relative to [OIII] $\lambda 5007$ implies $T_e > 50,000$ K, which is incompatible with photoionised low-density clouds ($n_e \sim 10^2 - 10^4$ cm $^{-3}$). He suggested that this dilemma vanishes if relatively dense clouds ($n_e \simeq 10^6 - 10^7$ cm $^{-3}$) exist in the narrow line regions. (See also Filippenko & Halpern 1984.) We suggest that in our model the high density contribution to the [OIII] line comes from the ILR while the NLR densities are similar in all AGN.

(ii) Surveys:

(a) Francis et al (1992) applied principal component analysis to a QSO sample taken from the Large Bright QSO survey and found that three principal components account for approximately 75% of the intrinsic variance in the sample. The analysis supports a two-zone line emitting model with a BLR and an additional region producing the line core, $\text{FWHM} \sim 2500 \text{ km s}^{-1}$. They point out that this line core region is not the traditional NLR.

(b) Van Gröningen and de Bruyn (1989) found broad wings in $[\text{OIII}]\lambda 5007$ in 10 out of 12 objects in their sample of Seyfert 1 galaxies. From the ratio to $[\text{OIII}]\lambda 4363$ and $\text{H}\beta$ in 4 of the 10 they deduced the existence of a transition zone intermediate between the BLR and NLR with a mean density of $5 \times 10^6 \text{ cm}^{-3}$ at a minimum radius of 0.8 pc.

(c) Wills et al. (1993) investigated 123 high luminosity AGN. They found that the CIV profile consists of a core with characteristic width of approximately 2000 km s^{-1} FWHM plus a broad base component. The core component is attributed to an ILR.

(d) In those cases where they could measure strong wings Brotherton et al. (1995) used principal component analysis on the $\text{H}\beta$ profiles of 41 radio-loud quasars and found that the second most significant variation in this emission line appears to involve an intermediate width ($\sim 2000 \text{ km s}^{-1}$) component with a small redshift. The strength of this component is correlated with the strength of $[\text{OIII}]\lambda 5007$.

(iii) The narrow lines:

Narrow emission line asymmetry is observed in most Seyfert 1 and Seyfert 2 galaxies. The narrow line profiles in these objects are usually smooth with a clear tendency for the blue wing of some lines to be stronger. This blue asymmetry is most noticeable in lines of higher excitation or critical de-excitation density. Also, the higher excitation lines are usually found to be broader and more blueshifted than the low excitation lines (Whittle 1985, 1988). In our model such asymmetries may be explained, at least in general qualitative terms, by contributions from the ILR to the narrow emission lines.

This ILR contribution to the narrow lines might also be the reason for differences observed in the spread of line profile shapes in a given object, Σ , in a sample of Seyfert galaxies. Whittle (1988) found that Seyfert 1s have high Σ , Seyfert 2s low Σ while intermediate Seyferts have values in-between. Whittle (1985) suggested that galaxy or bulge mass may be the important underlying variable but in the later paper (1988) could find no correlations between line profile variations and host galaxy properties. The observed trend was accounted for in a two component picture of the NLR (Mobasher & Raine 1989), similar to the NLR/ILR picture considered here in as much as the second component provides the higher velocity, higher density material.

Whittle also found a lack of correlation between $[\text{OIII}]$ line width and the nuclear nonthermal luminosity, the strength of the BLR or the ionisation and physical state of the NLR gas. For the Seyfert 1 sample, however, correlations were found between broad ($\text{H}\alpha$ and $\text{H}\beta$) and narrow ($[\text{OIII}]$) line widths. The correla-

tion with $[\text{OIII}]$ is stronger with the broad-line core widths than with the broad-line wings. Similarly, the broad line widths are more strongly correlated with the narrow line base widths than the narrow line core widths (Whittle 1985; Wilson & Heckman 1985). In our model a significant contribution to the broad-line core emission comes from the ILR as do the base widths of the higher critical density narrow lines (particularly $[\text{OIII}]$). So we expect a correlation between the narrow line widths and the broad-line core widths and between narrow line base widths and broad-line widths. The ILR emission provides a possible basis for a simple explanation of these observations and the lack of correlation between line profile differences and host galaxy properties. Absence (or obscuration) of the ILR in NLRGs might also provide an explanation for the mismatch of the $[\text{OIII}]\lambda 5007$ emission in BLRGs and NLRGs, while the $[\text{OII}]\lambda 3727$ luminosities (which come only from the NLR) in these galaxies match each other well (Hes et al. 1993).

5.4.1. Coronal lines

Coronal lines are forbidden transitions within the ground terms of highly ionised species ($h\nu_{ion} \gg 100\text{eV}$) (Oliva et al. 1994) which can be formed either by a hard UV photoionising continuum (Grandi 1978; Korista & Ferland 1989) or in a hot ($T \sim 10^6\text{K}$) collisionally ionised plasma (Oke & Sargent 1968; Nussbaumer & Osterbrock 1970). A combination of shocks and photoionisation has also been suggested (Viegas-Aldrovandi & Contini 1989).

The $[\text{Si VI}]\lambda 1.962$ line seems to be associated with the active nucleus as this line is found in Seyferts but not in starburst galaxies (Marconi et al 1994). Spinoglio & Malkan (1992) placed the coronal line region just outside the BLR. Thompson (1995) considers that in NGC 4151 the coronal lines arise near the interface between the dusty torus and the BLR mainly on account of the large line widths. The critical density for the $[\text{Si VI}]$ line at $1962 \mu\text{m}$ is $\sim 10^8 \text{ cm}^{-3}$ (Greenhouse et al. 1993; Oliva & Moorwood 1990). In our model these densities are associated with the ILR, the dispersing BLR clouds and shocked material in the BLR. Since the $[\text{Si VI}]$ line widths span a large range (Giannuzzo et al 1995), from very narrow profiles ($\text{FWHM} \sim 300 \text{ km s}^{-1}$) to widths approaching those of the broad lines, the main contribution to the $[\text{Si VI}]$ line may come mainly from different regions in different galaxies.

6. A unified AGN model

We have so far seen that viewed at various angles our picture of NGC 4151 gives rise to obscured Seyfert 1s with a range of obscuring columns, a class of intermediate Seyferts and Seyfert 1s with varying degrees of partial covering and absorption of the X-ray source and unobscured Seyfert galaxies. We now wish to apply the model to objects at lower and higher luminosities than those attained in the various states of NGC 4151. We therefore need to know how the intrinsic structure varies with luminosity. There are at least two predictions relevant to a unified model. These are that both the disc flaring and the injection of cloud

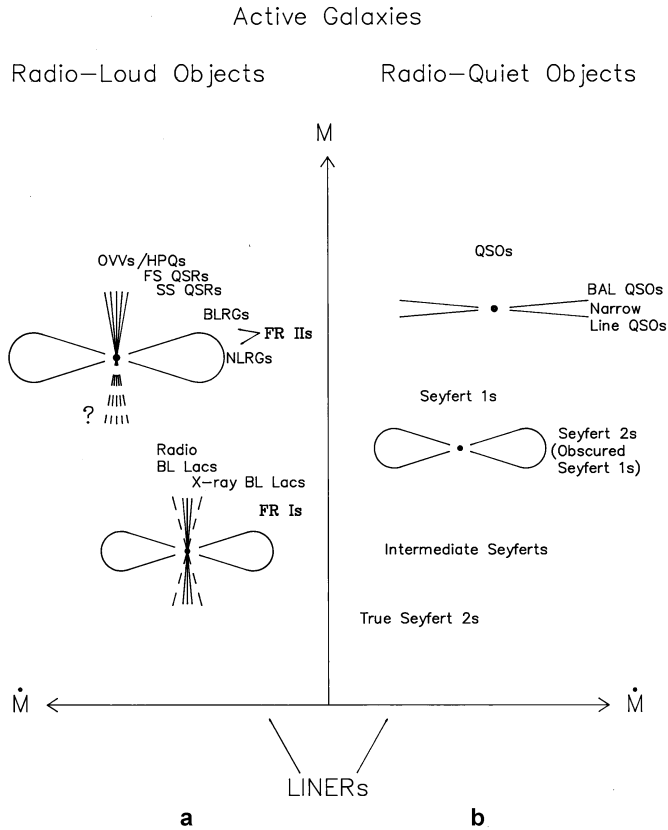


Fig. 4. **a** High and low luminosity radio-quiet AGN as seen from various lines of sight. **b** High and low luminosity radio-loud AGN as seen from various lines of sight.

material from the disc are functions of luminosity. For the latter we can adapt the discussion of Smith and Raine (1985, 1988, following Begelman et al. 1983): external illumination drives a thermal disc wind which here fuels the ILR (not the BLR as in our earlier papers); for an incident luminosity $L/L_{Edd} < 0.03T_8^{1/2}$, where T_8 is the Compton temperature of the incident radiation in units of 10^8K , a strong disc wind does not form and we expect there to be little or no ILR gas. We have already seen that the BLR clouds are not present at low luminosity in a source with time varying luminosity.

Fig. 4 shows our extension of the unified picture beyond the range of luminosities appropriate to NGC 4151. We summarise it here and give more details in the following sections. It is reasonable to assume that a steady high luminosity is associated with high wind power. Then we predict that the disc in the BLR does not flare at high luminosity (Sect. 6.1). Thus there are no NGC 4151-like absorption systems in high luminosity objects, but we get instead, at the right viewing angle, the broad absorption line quasars (BAL QSOs). At low steady luminosity the BLR survives, but the ILR does not. We also expect (although we do not show here) that the absence of a flared disc exposes the dust region to the full force of the nuclear wind, giving rise to strong shocks (in the wind and the dusty material) and strong heating. Therefore the dust obscuration is less important

at high luminosity. The fraction of obscured systems should therefore decrease with increasing continuum power. The model is consistent with a luminosity sequence: LINERs, True Seyfert 2s, Intermediate Seyferts, Seyfert 1s, QSOs.

Note that the similar upturns in the near infrared that is seen in almost all quasars and Seyferts is evidence for similar covering factors of dust in these systems. This is supported by the fairly small range in the relative sizes of the blue bump and the infrared bump found by Sanders et al. (1989) in 109 bright quasars in the PG survey. This is compatible with our picture, because the flux falling on the disc is only weakly dependent on its shape: a disc flattened by a significant wind will experience less direct irradiation but a larger component due to scattering in the wind. We find an effective covering factor that is therefore always in the region of 10%.

6.1. Luminosity dependence of the model

We compute first how the disc flaring depends on luminosity assuming a steady state. Let the angle between the radius vector to a point on the disc surface and the tangent vector at that point be α . If the ram pressure in the radially flowing wind is P_m then the interaction with the disc destroys momentum normal to the disc surface at a rate $P_m \sin \alpha$ per unit area. But the average pressure on the disc surface is fP_m where $f \sim 3 \times 10^{-3}(L/L_m)$, omitting factors of order unity, $\sim 10^{-4}$ (Cassidy and Raine 1996). Thus $f = \sin \alpha$ where, if $z = z(r)$ is the disc surface as a function of radius r in the disc,

$$\alpha = \tan^{-1}(dz/dr) - \tan^{-1}(z/r).$$

Taking the small angle approximation therefore gives for the disc surface

$$\frac{dz}{dr} - \frac{z}{r} = f$$

or

$$z = (h_0/r_0 + f \log(r/r_0))r$$

where h_0 is the disc height at some reference point r_0 . In this region the disc height increases close to linearly with radius.

As we move out further in the BLR region, beyond a radius r_* (say), the momentum extracted from the wind to accelerate the clouds cannot be neglected. The loss of momentum in an element of wind as it entrains clouds at the disc surface between r and $r + dr$ is proportional to the mass injection rate in clouds, $d\dot{M}/dr$, and inversely proportional to the residence time in the element, v_n/\dot{v} . Since (see Cassidy & Raine 1996) $d\dot{M}/dr \propto 1/r$ and the cloud acceleration, $\dot{v} \propto 1/r^2$ we have, in this region, $r > r_*$, that the actual ram pressure of the wind, P'_m , is

$$P'_m \propto r^{-3} = P_m r_*/r.$$

Thus, the disc pressure, which by definition is fP_m , must now balance $\sin \alpha P'_m$, from which we derive, as above,

$$z = r[h_{BLR}/r_{BLR} + f(r - r_{BLR})/r_*],$$

where h_{BLR} is the height of the disc at the outer edge of the BLR. We take this as a scale height at r_{BLR} . Therefore, in this region the disc rises more strongly into the wind in order to balance the pressure of heated material at the surface and the surface flares until it reaches a scale height at the outer radius of the BLR. Clearly the radius, r_* , at which the disc begins to flare will be larger, for a given mass loss rate in clouds, the larger the momentum in the wind. Provided the momentum flux in the wind increases with the luminosity of the source more strongly than linearly (which we know to be the case in NGC 4151 from the line profile variations) then r_* will increase with luminosity until at high luminosity the disc does not flare at all and the BLR merges directly into the ILR. We see this as follows.

At the transition radius r_* we have, neglecting logarithmic terms,

$$h_* = r_*[h_{BLR}/r_{BLR} + f(r_* - r_{BLR})/r_*] \sim h_0 r_*/r_0.$$

Solving for r_* we get

$$r_* = r_{BLR}[1 - (h_0/r_0 - h_{BLR}/r_{BLR})(1/f)]^{-1} \\ \sim r_{BLR}^2 f / h_{BLR}.$$

We have $h_{BLR} \propto r_{BLR}^{3/2}$ for an isothermal disc, and $r_{BLR} \propto (L_r^{3/2}/L_m)$, ignoring logarithmic terms (Cassidy and Raine 1996). Thus, finally,

$$r_* \propto (L/L_m)^{3/2},$$

and the flared region is smaller for higher luminosities.

A further consideration is the importance of radiation pressure acceleration of the clouds. For the acceleration, α_w , due to the wind, having speed $10^{10}v_{10}$ cm s⁻¹, and the acceleration due to radiation pressure for a completely absorbing cloud, α_r , we find the ratio

$$\frac{\alpha_r}{\alpha_w} = 0.3(L_r/L_m)v_{10}.$$

So, unless the energy flux in the wind is comparable with that in radiation, radiation pressure driving is important. Since radiation pressure and ram pressure have the same radial dependence this makes no difference to the line profiles, except that changes in luminosity are now linked directly to changes in profile width, rather than through assumptions on the relation between the momentum carried by the wind and by the radiation field. (For NGC 4151 our profile fit in the high state gave $L_r/L_m = 0.2$ so radiation pressure acceleration is unimportant. It may be significant in lower luminosity states since L_r/L_m increases as L_r decreases.)

6.2. Lower luminosity systems

The sub-class of LINERs that are the lowest luminosity AGN (Heckman 1986) appear in our model at low values of \dot{M} . (Note that we are concerned only with the *AGN-type* LINERs in the following, without prejudice to other types.) Over 1/3 of LINERs studied in a survey of intrinsically faint Seyfert nuclei have

detectably broad H α wings (FWHM a few thousand km s⁻¹), reminiscent of the broad emission lines that define type 1 Seyfert nuclei (Filippenko & Sargent 1986). Heckman (1980) had already pointed out that many LINERs appear to form a natural extension of Seyfert 2 galaxies to smaller values of [OIII]/H β . Moreover, the narrow emission lines in a given nucleus often have markedly different widths as observed in the NLRs of Seyferts. For example, [OI] λ 6300 is far broader than the [NII] and [SII] lines in the nucleus of M81. The [OI] line has $n_{crit} \sim 1.4 \times 10^6$ cm⁻³, whereas the much narrower [SII] λ 6726,6731 lines have $n_{crit} \sim 2.1 \times 10^3$ cm⁻³. This confirms that the gas density in the NLR in LINERs is increasing with decreasing distance from the centre (Filippenko & Halpern 1984) in the same way as in the NLR of Seyferts (see Whittle 1988). Further evidence for a mini-Seyfert nucleus at the centre of LINERs comes from observations of NGC 1097 by Storchi-Bergmann et al. (1993). They found that recently broad double-peaked H β and H α components appeared in the spectrum of the LINER.

For the lower luminosity systems our model predicts that with highly *variable* luminosities the BLR clouds will be wholly or partially absent in low luminosity states. This is because the inner radius of the BLR depends on the ratio of the current accretion power output to the local accretion rate; if this is small then the external illumination does not affect the disc and no BLR clouds are formed (Cassidy & Raine 1996). It also predicts, however, that in steady systems the BLR is always present, but that the ILR will be weak or absent below about $l_r = 0.03L_{Edd}$ at which the inner and outer radius of the thermally driven disc wind coincide (Begelman et al. 1983). Thus we distinguish between those Seyfert 2s that are really hidden type 1s and ‘genuine’ type 2s. In hidden type 1s the BLR will be obscured and the ILR may be. In true type 2s, for the most part, we expect both the BLR and ILR to be absent, but the population of these will be rare if variability decreases with decreasing luminosity.

Calculations by Ferland & Netzer (1983) and Halpern & Steiner (1983) indicate that LINER-like spectra could indeed result from reducing the luminosity of a Seyfert-like power-law continuum source by factors of 10-100 without changing the gas density or volume. We expect such an appearance for our steady-state unobscured low-luminosity systems.

6.3. Higher luminosity systems

At the highest luminosities we expect a Seyfert nucleus to be classified as a QSO. We expect the BLR to merge into the ILR, since the inner radius of the ILR is independent of luminosity whereas the outer radius of the BLR increases directly with luminosity (for a fixed black hole mass). We have seen that the flared region of the disc is no longer present at high luminosity so it will be necessary to calculate the effect of the nuclear wind impacting on the obscuring torus. We speculate that this leads to a deposition of energy in the torus (e.g. by shock heating) which will erode the dust at higher latitudes. Therefore we expect obscuration to be less likely in high luminosity objects. So

we expect few narrow line QSOs (high luminosity analogues of obscured Seyfert 1s).

Instead, viewed from close to the disc, the continuum and inner clouds are covered by the nearside outer broad-line clouds. These clouds are accelerated to high velocity in the line of sight and so give rise to broad absorption lines. These systems are therefore the BAL QSOs (see Sect. 6.4). The BAL QSOs are the high luminosity analogues of NGC 4151 and should therefore show complex X-ray absorption. Because the outer clouds are at larger radii in QSOs they have lower density and longer sound-crossing (or survival) times. Consequently we expect line absorption to be relatively more common in QSOs than in Seyferts.

Since the cloud debris is present at all luminosities, at appropriate angles X-ray absorption by warm material should be observed. Warm absorption has been observed in QSOs with the absorbing material being close to the central source (Pan et al. 1990). X-radiation falling on the disc, either directly or by scattering in the wind, will still be reprocessed by dust at low latitudes, so we do not expect large differences in the reprocessed infrared.

At luminosities high enough that the BLR disc is non-flaring the width of the CIV line is an orientation indicator (in radio-quiet objects).

6.4. Broad absorption line quasars

About 10% of all radio-quiet QSOs possess very broad absorption features (BAL QSOs, or BALs). Usually these are explained by broad-line clouds moving in front of each other and the source in certain lines of sight and therefore it is generally assumed that all QSOs possess a BAL region. The close similarity between emission line and continuum properties of QSOs and BALs (Weymann et al. 1991) is also consistent with the view that BALs do not form an intrinsically different class of QSOs. Broad absorption is mainly found in high ionisation resonance lines (eg. NV, CIV), while it is weak or absent in MgII. The broad absorption lines possess the following relevant properties:

(i) They often appear detached from the emission peak, but usually set in by the time an outflow velocity of 5,000 to 10,000 km s⁻¹ is reached.

(ii) The absorption profiles differ widely in terms of outflow velocity, level of ionization, velocity structure in the absorption troughs and strength of absorption (Turnshek 1987).

Observations also indicate that we are looking at material which has been accelerated radially outward (there are no red absorption troughs in BALQSOs) and that the absorbing material is situated fairly close to the quasar nucleus.

An important property of BALs is that they are all radio-quiet. Also, the optical polarisation properties in BALs appear to differ markedly from other radio-quiet QSOs, with BAL QSOs having a high probability of exhibiting significant polarisation (Turnshek 1987).

In his unified model Barthel (1989, 1991) associates the BAL regions with the weak radio jets of radio-quiet quasars. He suggests that BALs are viewed at small angles - the observer

looks at the jet - but are otherwise ‘normal’ QSOs. The problem is that, with a single jet-like geometry, it is difficult to produce the observed symmetric NV broad emission lines, for example by resonance scattering (Turnshek 1987); i.e. the NV line should be asymmetric.

The broad profiles and the large range of different profile widths in BAL QSOs are not compatible with a face-on disc in our BLR model since the emission lines from flat face-on discs are comparatively narrow with no large differences in widths between various objects. The observed BAL properties are, however, compatible with edge-on discs. At small inclinations to the disc plane the outer BLR clouds may shield some of the inner clouds and the continuum source from our view.

Note that broad absorption lines are less likely with a flared disc (because the BLR is hidden at most angles for which the shielding would occur), although the blue absorption feature in CIV for the special lines of sight to NGC 4151 and NGC 3516 arises from such shielding in our picture. The narrowness of the absorption dips in these objects results from the small BLR size and flaring of the disc. The smaller BLR size in Seyfert galaxies can also explain the correlation between the absorption troughs and the continuum intensity in these objects, which is not normally observed in BAL QSOs.

Our model predicts Seyfert-like absorption profiles (as opposed to BALs) for radio-loud BLRGs, where the BLR is in the line of sight. This should apply even to the most luminous objects because the disc should always be flared in radio sources (Sect. 7).

In our model the outer BLR clouds in QSOs are strong emitters of MgII, whereas CIV is mainly produced in the inner part. We therefore do not expect to see many broad MgII absorption systems. Also, we expect a difference in the absorption velocities of CIV and MgII. Both these predictions are confirmed by observations: MgII absorption is found in only ~ 15% of all BAL QSOs and where present it is generally less extensive in velocity space than CIV (Woltjer 1990). The geometry of BAL quasars predicted by our model agrees in general with the picture proposed by Turnshek (1987).

Voit et al. (1993) estimate that the BAL clouds have equivalent hydrogen column densities $\sim 5 \times 10^{21} \text{ cm}^{-2}$ to 10^{23} cm^{-2} and ionisation parameter, $U \sim 0.1 - 1.0$, where U is given in terms of the luminosity, distance and cloud density (cm^{-3}) as $U = 10^8 L_{46} / n R_{pc}^2$. These estimates are within the range of values for the outer BLR and ILR of the disc-wind picture. In addition, in our model of NGC 4151 we ignored radiation pressure acceleration of the clouds. Since the radiative driving force, like that due to ram pressure, falls off as $1/r^2$ the inclusion of radiation pressure makes no difference to the agreement between the model and observation except that it makes it impossible to determine a unique set of wind parameters. There is therefore no conflict between our results and the conclusions of Arav et al. (1995) on the role of radiative acceleration in the BAL region. Our picture for BAL QSOs is similar to those proposed recently by (Goodrich & Miller 1995; Cohen et al. 1995), except that we associate the BAL region with the outer BLR.

Nevertheless there remains a significant problem for *all* theories of the BAL region, namely the apparently very high metal abundances compared to solar, and, by implication, to the BLR (Turnshek et al 1996). To some extent some of these abundances are model dependent (for example on a one- or two-component photoionisation model), so it remains to be seen if they persist to the same extent in our stratified picture. If they do, then they imply either a large abundance gradient across the BLR, which may not be compatible with the emission line ratios, or that the BAL gas cannot be identified with the BEL gas and hence that BALs are a separate class. However, this would not solve the problem for us, since it would leave us with a class of edge-on objects that apparently has no observational counterpart. BALs therefore seem to provide a crucial test for the model we are proposing.

7. Radio loud objects

The infrared to soft X-ray continua, as well as the optical and UV properties of lobe-dominated radio source and radio-quiet AGN are generally similar (Sanders et al. 1989). This is a strong indication that they are produced in the same way and that the quest for a unified picture of radio-loud and radio-quiet objects is not a lost cause. The basic starting point for our unified model with regard to radio-loud sources is therefore that these are the radio-quiet systems with a radio jet added in each case. Thus we ignore, at least in the first instance, any interaction between the radio jet, or jet emission, and the other structures in the model.

Of course, the properties of the radio emission itself may depend on the radio luminosity, as indeed it does. We recognise two luminosity classes (Fanaroff and Riley 1974): the edge-darkened FRI sources with radio power $< 10^{25.3} \text{W Hz}^{-1}$ and the edge brightened FRII sources with radio powers $> 10^{25.3} \text{W Hz}^{-1}$. Since we are assuming the radio and BLR properties are independent, this classification does not affect our hypothesis that the radio quiet and radio loud systems should form parallel series. Our point in this section is that the adoption of our series for the radio-quiet systems overcomes some of the problems in achieving this parallelism within the ‘SPM’ unified scheme.

We adopt the angle dependence of the usual unified picture for radio-loud systems (see Urry & Padovani 1995 for a review) since the structure of the radio jet gives a good indication of the angle to the line-of-sight. However there should be present amongst radio-loud systems the analogues of the ‘true’ Seyfert 2s and the obscured Seyfert 1s. The latter class has a representative in 3C 234 in which the broad lines were detected in polarised light before those in NGC 1068 (Antonucci & Cohen 1983).

Barthel (1989, 1991), in his unified scheme, stipulates that quasars and radio galaxies have the same relation as Seyfert 1 and Seyfert 2 galaxies with the central quasar in the narrow line radio galaxies obscured by an absorbing torus. One of the difficulties with Barthel’s model is this: Laing et al. (1993) studied a complete subsample of 3CR radio sources with $z < 0.88$ and found two classes of FRII narrow-line spectra: low and high excitation. Within the high-excitation spectra they find comparable numbers of objects with and without detectable broad lines at all

redshifts. These fit into Barthel’s unified scheme. They detect no broad lines in the low-excitation objects, but a few objects show strong radio cores and other indications of beaming. For the low-excitation group they therefore suggest a picture more reminiscent of the BL Lac/FR I unified scheme (Blandford & Rees 1978; Browne 1983; Antonucci & Ulvestad 1985; Urry et al. 1991).

Murphy et al. (1993) found that BL Lac objects are not more core-dominated than the quasars in a well-defined sample of powerful radio sources. They find no evidence that BL Lacs are those quasars seen at such small angles to the line of sight that the relativistically beamed core emission swamps that from other components, and come to the view that the majority of BL Lacs are related to the low-luminosity FRI radio galaxies. However, they observed a substantial fraction of BL Lac objects with extended radio emission with powers and structures more characteristic of FRIIs. These FRII-luminosity BL Lacs are difficult to account for in the context of the standard unified scheme (although if the radio axis were a function of time this could account for the extended emission). One of the suggestions of Murphy et al., namely that the BL Lacs know nothing of the FRI-FRII division and can be beamed versions of either type of radio source, fits into our picture.

In our model the structure of the BLR is independent of radio power. This implies that the cut-off in cloud production in the BLR, that is, the classification of radio-loud objects with or without broad lines, must be independent of the transition between FRII and FRI objects. As a consequence we expect to observe either FRIIs without BLRs or FRIIs with BLRs. Note that the model predicts an inner BLR radius $\propto T_c^{-1/3}$ (Cassidy & Raine 1996) so if the steep X-ray spectrum implies a Compton temperature, T_c as low as 10^6K for the radiation falling on the disc then the BLR will be largely absent. The observation of relatively narrow broad wings to $H\alpha$ in a number of BL Lacs does not imply the existence of a BLR as these can arise in the ILR. (We expect that at least the higher luminosity FRII/BL Lacs still possess their ILRs.) Hence FRII-luminosity BL Lacs could represent our FRIIs with absent BLRs and would be the radio-loud true Seyfert 2 analogues.

Another problem concerns the BAL QSOs: they appear to have no radio loud analogues. Such analogues would be expected in a spherically symmetric picture where broad absorption lines from clouds in the line of sight, are uncorrelated with the radio axis. But we do find Seyfert type absorption in radio loud systems. This points to a picture in which, contrary to our initial hypothesis, the radio jet and disc structure are correlated to the extent that the presence of the radio jet rules out the possibility of a flattened disc. Such a correlation would be entirely natural (although not proven) in our picture. Recall that the disc flaring is suppressed at high luminosity (= high wind power) by the disc-wind interaction. In radio-loud systems it would be natural to suppose that the momentum carried away in the jet is not available in the nuclear wind. Hence the nuclear wind carries insufficient momentum to suppress the disc flaring. So we expect to see some flaring of the accretion disc even in the highest luminosity radio-loud objects. This is also indicated by the

existence of high luminosity NLRGs. The disc flaring also settles the question of why the high luminosity blazars and QSRs, which are viewed face-on, or close to face-on, do not show relatively narrow broad emission lines as would be expected by comparison with the face-on QSOs (Sect. 5.1).

Wills and Brotherton (1996) attributed the existing differences in the optical-UV spectra between radio-loud and radio-quiet objects to two apparently independent relations: (i) For radio-loud quasars, with increasing core dominance, emission lines are narrower, FeII emission is stronger, and CIV has stronger red wings. With decreasing core-dominance, H β more often has stronger red wings, and the likelihood of associated absorption and reddening increases. (ii) For radio-quiet objects there is an inverse relation between the strengths of FeII and [OIII] λ 5007 emission, with the strong FeII-weak [OIII] QSOs being associated with low ionisation BALs, reddening and polarisation.

We can explain these observations as follows:

(i) the narrowing of the emission lines with increasing core-dominance is due to the disc-like distribution of the BLR clouds. CIV has stronger red wings because the CIV cloud profile is symmetric for face-on objects but the reflected component boosts the red wing. The increase in FeII emission can be explained if FeII arises in the accretion disc (e.g. Joly 1991). That the likelihood of absorption and reddening increases with decreasing core-dominance is evident when considering Fig. 1. At present we cannot explain why H β more often has stronger red wings with decreasing core-dominance.

(ii) We would expect an increase in reddening and polarisation for edge-on objects (Sect. 6.7). The weak [OIII] λ 5007 emission in low ionisation BAL QSOs and the strong FeII emission from edge-on radio-quiet objects (contrary to the trend in radio-loud quasars) is more difficult to explain. However, weak [OIII] is not sufficient to predict the presence of BALs; there are examples of strong [OIII] emitters amongst BAL QSOs (Turnshek 1995). We can speculate that the difference in FeII is associated with the different structure of the accretion discs.

In Fig. 4(b) we show the radio-loud analogues of QSOs and Seyferts at high and low luminosity and their classification when viewed from various angles. For completeness we summarise briefly here what this picture shows, although none of the following is new. At the high luminosity end we have OVV's and HPQs, radio-loud quasars and FRIIs. OVV's and HPQs are observed when we look directly at the jet. At larger cone-opening angles we observe flat-spectrum (core-dominated) and steep-spectrum (lobe-dominated) QSRs. At even larger angles we have broad-line radio-galaxies. Objects where the BLR or BLR and ILR are obscured by the disc are narrow-line radio galaxies (NLRGs).

At the lower luminosity end we have BL Lacs and FR I radio galaxies. The idea is that FR I radio galaxies have relativistic jets (this is not yet proven) in which nonthermal emission, when viewed from small angles, dominates the emission of the galaxy. They are the parent population of BL Lacs (Blandford & Rees 1978; Blandford & Königl 1979; Orr & Browne et al. 1982; Browne 1983; Wardle et al. 1984; Antonucci & Ulvestad 1985; Sarazin & Wise 1993). At even lower luminosities we have

radio-loud LINERS. Most of the AGN-type LINERS found in bright, nearby galaxies are associated with weak compact radio sources; however, some LINERS have been found in the nuclei of powerful radio galaxies, eg. M87 (Goodrich & Keel 1986).

An interesting suggestion was made by Falcke et al. (1995, 1996). They stipulate that the flat spectrum radio intermediate quasars are actually boosted radio-quiet objects. This implies the assumption that radio-quiet objects also have relativistic jet, but a factor of ~ 100 - 1000 less luminous than the radio-loud objects. If this is correct then flat spectrum quasars should appear in Fig. 4a as face-on QSOs and not in Fig. 4b. Our model then predicts that these objects will have relatively narrow broad emission lines.

8. Conclusions

We begin by summarising the way in which the picture we have presented in this paper differs from the molecular torus unified model. The torus at large radii obscures the direct view of the BLR and material from the torus provides the scattering medium by which the BLR is indirectly visible. The torus is also responsible for the beaming of the UV. There is a fixed cone opening angle which is not in agreement with observation. Modifications to this must be made ad hoc.

In our picture the BLR clouds themselves sustain the scattering medium. Except at high luminosity (assuming this implies a high mass outflow) the disc flares in the BLR, partially collimating the nuclear outflow away from the disc plane. At larger radii a ring of dusty material (possibly associated with the disc) then provides an obscuring screen. At high luminosity the disc flaring is suppressed and the presence of a strong wind close to the disc plane removes the obscuring ring (leaving a geometrically thin, opaque, dusty disc). The angle subtended by the scattering cone will in general be different from the UV cone. The obscuring cone depends on luminosity in a predictable way, through the disc flaring, in general qualitative agreement with the data. The model for the different luminosity states of NGC 4151 at a fixed angle can be extended to describe other active nuclei of various luminosity classes at different angles.

A unified model based on NGC 4151 as archetype leads to the following conclusions. (But note we are not claiming it is the only model that can do so.)

1. Principally as a result of the non-spherical BLR geometry
 - (a) there is no conflict between the Hubble data and the alignment of the UV cone and radio structure in NGC 4151;
 - (b) a range of X-ray columns are possible with, depending on the line of sight, partial covering in some cases and warm absorbers in others (and, in the case of NGC 4151, both).
 - (c) there are no BAL Seyferts or radio loud BAL quasars.
2. As a consequence of a luminosity dependent BLR, (possible because the ram pressure accelerated clouds are short-lived):
 - (a) there are nuclei that appear (for an inflow timescale, $> 10^5$ years) as true Seyfert 2s with low X-ray absorption;

- (b) classification changes in Seyferts are possible on short time scales (weeks to months).
3. The luminosity dependence of the disc flaring and obscuration means that the picture is compatible with
- the lack of evidence for obscuring dust in some Seyfert galaxies (or positive evidence that it is not there);
 - the possibility that there are no high luminosity Seyfert 2s (assuming that the IRAS galaxies are young QSOs that have recently switched on);
 - variations in opening angle of the obscuring torus, which are implied by observations, and also required if Seyfert galaxies are not to overproduce the X-ray background (Mulchaey et al. 1992).
4. The contribution of the ILR to the ‘narrow’ line emission, implies that
- there is no missing [OIII] $\lambda 5007$ problem in some NLRGs and BLRGs;
 - the NLR profiles in galaxies classified observationally as lower luminosity Sy2s, should show no evidence for any ILR component. This is at least consistent with the similarity of profiles for different lines within these systems.
 - the problem of assigning a consistent temperature from [OIII] $\lambda 4363$ in photoionisation models is resolved.
 - the [OIII] $\lambda 5007$ line can have a blue wing without the need to invoke NLRs with high densities.
5. Finally, the combination of BLR geometry and short-lived BLR clouds means
- the NLR cone has a larger angular extent than the scattering cone (which is a conical shell).

NGC 1068 can be fitted into this picture because the exceptionally large column of dust it contains is special to its line of sight. (It may be associated with the equatorial plane of a star formation ring in the galaxy.) The model predicts a correlation between X-ray absorption and both high-ionisation forbidden line profiles and broad-line profiles, and a correlation between UV and X-ray absorption at certain angles. There should also be a relation between the luminosity function and profile width distribution for radio-quiet objects. Broad-line radio galaxies appear over a different range of angles from radio quasars and so should have broader lines on average. These may provide possible tests which we hope to discuss elsewhere.

Acknowledgements. We are grateful to Dave Smith for directing us to the X-ray data of Fig. 2 and guiding us in the use of XSPEC to analyse it, and to two anonymous referees for their constructive scholarship.

References

- Alloin, D., Pelat, D., Phillips, M., Whittle, M., 1985, *Astrophys. J.*, 288, 205
- Andrillat, Y. & Souffrin, S., 1968, *Astrophys. Lett.*, 1, 111
- Antonucci, R.R.J., Cohen, R.D., 1983, *Astrophys. J.*, 271, 564
- Antonucci, R.R.J., 1984, *Astrophys. J.*, 278, 449
- Antonucci, R.R.J., 1993, *Ann. Rev. of Astron. Astrophys.*, 31, 473
- Antonucci, R.R.J., Ulvestad, J.S., 1985, *Astrophys. J.*, 294, 158
- Antonucci, R.R.J., Hurt, T. & Miller, J., 1994, *Astrophys. J.*, 430, 210
- Arav, N., Korista, K.T., Barlow T.A. & Begelman M.C., 1995, *Nature*, 376, 576
- Baker, J.C. & Hunstead, R.W., 1995 *Astrophys. J.* 452, L95
- Barr, P., Willis, A.J. & Wilson, R., 1983, *MNRAS*, 203, 201
- Barthel, P.D., 1989, *Astrophys. J.*, 336, 606
- Barthel, P.D., 1991, *Physics of Active Galactic Nuclei*, eds. W.J. Duschl and J.S. Wagner, Springer Verlag, p. 637
- Begelman, M.C., McKee, C.F., Shields, G.A., 1983, *Astrophys. J.* 271, 70
- Blanco, P.R., Ward, M.J., Wright, G.S., 1990, *MNRAS*, 242, 4P
- Blandford, R.D. & McKee, C.F., 1982, *Astrophys. J.*, 255, 419
- Blandford, R.D., Rees, M.J., 1978, in *Pittsburgh Conference on BL Lac Objects*, p. 328, ed. A. Wolfe
- Blandford, R.D. & Königl, A., 1979, *Astrophys. J.*, 232, 34
- Boller, T., Brandt, W.N. & Fink H., 1996, *Astron & Astrophys.*, 305, 53
- Boyle, B.J. & di Malteo, T., 1995, *MNRAS*, preprint
- Bregman, J.N., 1991, *Physics of Active Galactic Nuclei*, eds. W.J. Duschl and S.J. Wagner, Springer Verlag, p. 699
- Bromage et al., 1985, *MNRAS*, 215, 1
- Brotherton M.S., Wills, B.J., Francis, P.J. & Stendal, C.C., 1994, *Astrophys. J.*, 430, 495
- Brotherton, M.S., 1996, *Astrophys. J. Supp.*, 102, 1
- Browne, I.W.A., et al., 1982, *MNRAS*, 198, 673
- Browne, I.W.A., 1983, *MNRAS*, 204, 23P
- Capetti, A., Axon, D.J., Maschetto, F., Sparks, W.B. & Boksenberg, A., 1995, *Astrophys. J.*, 446, 155
- Cassidy, I., Raine, D.J., 1993, *MNRAS*, 260, 385
- Cassidy, I., Raine, D.J., 1996, *Astron. Astrophys.* 310, 48
- Clement, R., Sembay, S., Hanson, C.G., Coe, J.M., 1988, *MNRAS*, 230, 117
- Cohen, M.H., Ogle, P.M., Tran, H.D. Vermeulen, R.C. 1995, *Astrophys. J.* 448, L77
- Crenshaw, D.M., Peterson, B.M. & Wagner, R.M., 1988, *Astron. J.*, 96, 1208
- de Robertis, M., 1987, *Astrophys. J.*, 316, 597
- Done, C. & Krolik, J.H., 1996, *Astrophys. J.*, 463, 144
- Edelson, R.A. & Malkan, M.A., 1986, *Astrophys. J.*, 308, 59
- Efstathiou, A. & Rowan-Robinson, M., 1995, *MNRAS*, 273, 649
- Evans, I.N., Tsvetano, Z., Kriss, G.A., Ford, H.C., Caganoff, S. & Koratkar, A.C., 1993, *Astrophys. J.*, 417, 82
- Fahey, R.P., Michalitsianos, A.G., Kazanas, D., 1991, *Astrophys. J.* 371, 136
- Falcke, H., Gopal-Krishna, Biermann, P.L., 1995, *Astron. Astrophys.*, 298, 395
- Falcke, H., Sherwood, W., Patnaik, A.R., 1996, preprint
- Fanaroff, B.L., Riley, J.A., 1974, *MNRAS* 167, 31P
- Ferland, G.J., Netzer, H., 1983, *Astrophys. J.*, 264, 105
- Ferland, G.J., Peterson, B.H., Horne, K., Welsh, W.F. & Nahar, S.N., 1992, *Astrophys. J.*, 387, 95
- Filippenko, A.V., 1985, *Astrophys. J.*, 289, 475
- Filippenko, A.V., Halpern, J.P., 1984, *Astrophys. J.*, 285, 458
- Filippenko, A.V., Sargent, W.C.W., 1986, *Observational Evidence of Activity in Galaxies*, eds. E.Ye. Khachikian, K.J. Fricke & J. Melnick, p. 451
- Francis, P.J., Hewett, P.C., Foltz, C.B. & Chaffee, F.H. 1992, *Astrophys. J.*, 398, 476
- Giannuzzo, E., Rieke, G.H., Rieke, M.J., 1995, *Astrophys. J.*, 446, L5
- Giuricin, G., Mardirossian, F., Mezzetti, M., 1995, *Astrophys. J.* 446, 550
- Goodrich, R.W. & Keel, W.C., 1986, *Astrophys. J.*, 305, 148

- Goodrich, R.W. Miller, J.S. 1995, *Astrophys.J.*, 448, L73
- Grandi, S.A., 1978, *Astrophys. J.*, 221, 501
- Greenhouse, M.A., Feldman, U., Smith, H.A., Klapisch, M., Bhatia, A.K. & Barshalom, A., 1993, *Astrophys. J. Supp.* 88, 23
- Halpern, J.P., Steiner, J.E., 1983, *Astrophys. J.*, 269, L37
- Heckman, T.M., 1980, *Astron. Astrophys.*, 87, 142
- Heckman, T.M., Miley, G.K., Green, R.F., 1984, *Astrophys. J.*, 281, 525
- Heckman, T.M., 1986, *Observational Evidence for Activity in AGN*, eds. E.Ye. Khachikian et al., p. 421
- Heckman, T.M., Chambers, K., Schilizzi, R. & Postman, M., 1992, *Astrophys.J.*, 391, 39
- Heckman, T.M., O'Dea, C.P., Baum, S.A. & Laurikainen, E., 1994, *Astrophys. J.*, 428, 65
- Heckman, T.M. et al., 1995, *Astrophys. J.*, 446, 101
- Hes, R., Barthel, P.D., Fosbury, R.A.E., 1993, *Nature*, 362, 326
- Hutchings, J.P., 1987, *Astrophys. J.*, 320, 122
- Inda, M., Makishima, K., Kohmura, Y., Tahsiro, M., Ohashi, T., Barr, P., Hayshida, H., Palumbo, G.G.C., Trinchieri, G., Elvis, M., Fabbiano, G., 1994, *Astrophys. J.*, 420, 143
- Jijima, T., 1992, *IAU Circ.*, 5521
- Jijima, T., Rafanelli, P., Bianchini, A., 1992, *Astron. Astrophys.*, 265, L25
- Joly, M., 1991, *Astron. Astrophys.* 242, 49
- Kay, L.E., 1994, *Astrophys. J.*, 430, 196
- Kinney, A.L., Antonucci, R.R.J., Ward, M.J., Wilson, A.S., Whittle, M., 1991, *Astrophys. J.*, 377, 100
- Kollatschny, Fricke, 1985, *Astron. Astrophys.*, 146, L11
- Kwan, J., 1984, *Astrophys. J.* 283, 70
- Laing, R.A., Jenkins, C.R., Walls, J.V., Unger, S.W., 1993, Poster Paper presented at Mt. Stromlo Symposium in June 1993
- Lawrence, A., 1991, *MNRAS* 252, 586
- Loska, Z., Czerny, B., Szczerba, R., 1993, *MNRAS* 262, L31
- Maiolino, R., Ruiz, M., Rieke, G.H. & Keller, L.D., 1995, *Astrophys.J.*, 446, 561
- Maisack, M., Yaqoob, T., 1991, *Astron. Astrophys.*, 249, 25
- Maoz, D., et al. 1991, *Astrophys.J.*, 367, 493
- Marconi, A., Moorwood, A.F.M., Salvat, M., Oliva, E., 1994, *Astron. Astrophys.*, 291, 18
- Marshall, F.E. et al., 1993, *Astrophys.J.*, 405, 168
- Mathews, W.G. & Ferland, G.J., 1987, *Astrophys. J.*, 323, 456
- Mathews, W.G., 1993, *Astrophys.J.*, 412, L17
- McHardy, I. & Czerny, B., 1987, *Nature*, 325, 696
- Mobasher, B., Raine, D.J., 1989, *MNRAS* 237, 979
- Mulchaey, J.S., Mushotzky, R.F., Weaver, K.A., 1992, *Astrophys. J.*, 390, L69
- Murphy, D.W., Browne, I.W.A., Perley, R.A., 1993, *MNRAS*, 264, 298
- Nandra, K., Pounds, K.A., Stewart, G.C., Fabian, A.C. & Rees M.J., 1989, *MNRAS*, 236, 39
- Nandra, K. & Pounds, K.A., 1994, *MNRAS*, 268, 405
- Netzer, H., 1990, *Active Galactic Nuclei*, p. 57, *Swiss Society for Astrophysics and Astronomy*, eds. R.D. Blandford, H. Netzer, L. Woltjer, Springer Verlag
- Nussbaumer, H., & Osterbrock, D.E., 1970, *Astrophys. J.*, 161, 811
- Oke, J.B. & Sargeant, W.L.W., 1968, *Astrophys. J.*, 151, 807
- Oke, J.B., Redhead, A.C.S. & Sargeant, W.L.W., 1980, *PASP*, 92, 758
- Oliva, E. & Moorwood, A.F.M., 1990, *Astrophys. J.* 348, L5
- Oliva, E., Salvati, M., Moorwood, A.F.M. & Marconi, A., 1994, *Astron. Astrophys.*, 288, 457
- Orr, M.J.L., Browne I., 1982, *MNRAS* 200, 2067
- Pan, H.C., Stewart, G.C. & Pounds, K.A., 1990, *MNRAS*, 242, 177
- Pedlar, A., Howley, P., Axon, D. J. & Unger, S.W., 1992, *MNRAS*, 259, 369
- Penfold, J., 1992, *IAU Circ.*, 5533
- Penfold, J., 1992a, *IAU Circ.*, 5547
- Penston, M.V., et al. 1990, *Astron. Astrophys.* 236, 53
- Penston, M.V., Perez, E., 1984, *MNRAS*, 211, 33P
- Pogge, R.W., 1989, *Astrophys. J.*, 345, 730
- Pounds, K.A., Nandra, K., Stewart, G.C. & Leighley, K., 1989, *MNRAS*, 240, 769
- Pounds, K.A., Nandra, K., Stewart, G.C., George, I.M., Fabian, A.C., 1990 *Nature*, 344, 132
- Puchnarewicz, E.M., et al. 1992, *MNRAS*, 256, 589
- Reichert, G.A., Mushotzky, R.F., Petre, R., Holt, S.S., 1985, *Astrophys. J.*, 296, 69
- Reynolds, C.S. & Fabian A.C., 1995, *MNRAS*, 273, 1167
- Robson, E.I. et al. 1986, *Nature*, 323, 134
- Rodriguez Espinosa, J.M., Rudy, R.J., Jones, B., 1986, *Astrophys. J.*, 309, 76
- Rodriguez Espinosa, J.M., Rudy, R.J., Jones, B., 1987, *Astrophys. J.*, 312, 555
- Sanders, D.B., Phinney, E.S., Neugebauer, G., Soifer, B.T., Mathews, K., 1989, *Astrophys. J.*, 347, 29
- Sarazin, C.L., Wise, M.W., 1993, *Astrophys. J.*, 411, 55
- Shuder J.M., 1980, *Astrophys. J.*, 240, 32
- Smith, D.A. & Done, C., 1995, *MNRAS* (in press)
- Smith, M.J. & Raine, D.J., 1985, *MNRAS*, 212, 425
- Smith, M.J. & Raine, D.J., 1988, *MNRAS*, 234, 297
- Spinoglio, L. & Malkan, M.A., 1992, *Astrophys. J.*, 399, 504
- Stephens, S.A., 1989, *Astron. J.*, 97, 10
- Stürpe, G.M., van Gröningen, E., de Bruyn A.G., 1989, *Astron. Astrophys.* 211, 310
- Storchi-Bergmann, T., Baldwin, J.A., Wilson, A.S., 1993, *Astrophys. J.*, 410, 111
- Tadhunter, C. & Tsvetanov, Z., 1989, *Nature*, 341, 422
- Telesco et al 1984, *Astrophys.J.*, 282, 428
- Thompson, R.I., 1995, *Astrophys.J.*, 445, 700
- Tran, H.D., 1995, *Astrophys. J.* 440, 565
- Turnshek, D.A., 1987, *Proceedings of the QSO Absorption Line Meeting*, Baltimore, eds. J.C. Blades, D.A. Turnshek, C.H. Norman, p. 1
- Turnshek, D.A., 1995, in *QSO Absorption Lines* ed. G.Meylan, (Springer) 223
- Turnshek, D.A., Kopke, M., Monier, E., Noll, D., Epsey, B.R. & Weymann, R.J., 1996, *Astrophys. J.*, 463, 110
- Ulrich, M.-H., et al., 1984, *Astrophys. J.*, 382, 483
- Ulrich, M.-H., 1988, *MNRAS*, 230, 121
- Ulrich, M.-H. & Horne, K., 1996, preprint, *MNRAS*
- Ulvestad, J.S., 1986, *Astrophys. J.*, 310, 136
- Unger, S.W., Taylor, K., Pedlar, A., 1987, *Active Galactic Nuclei*, eds. D. Osterbrock, Miller, *IAU Symp.* 134, Kluwer Verlag, 331
- Urry, C.M., Padovani, P., Stickel, M., 1991, *Astrophys. J.*, 382, 501
- Urry, C.M. & Padovani, P., 1995, *PASP*, 107, 803
- van Gröningen, E. & de Bruyn, A. G., 1989, *Astron. Astrophys.*, 211, 293
- Viegas-Aldrovandi S., M. & Contini, M., 1989 *Astron. Astrophys.* 215, 253
- Voit, G.M., Weymann, R.J., Korista, K.T., 1993, *Astrophys. J.*, 413, 95
- Wamsteker, W., et al., 1985, *Astrophys. J.*, 295, L33 and L45
- Wamsteker, W. et al., 1990, *Astrophys.J.*, 354, 446
- Ward, M.J., et al., 1978, *Astrophys. J.*, 223, 788
- Warwick, R.S., Done, C. & Smith, D.A., 1995, *MNRAS*, 275, 1093

- Wardle, J.F.C., Moore, R.L., Angel, J.R.P., 1984, *Astrophys. J.*, 279, 93
- Weaver et al., 1994a, *Astrophys. J.*, 423, 621
- Weaver et al., 1994b, *Astrophys. J.* 436, L27
- Webster, R.L., Francis, P.J., Peterson, B.A., Drinkwater, H.J., Masci, F.J., 1995, *Nature*, 375, 469
- Weymann, R.J., Turnshek, D.A. & Christianson, W.A., 1985, in *Astrophysics of Active Galaxies and QSOs* ed. J.S. Miller, p333
- Weymann, R.J., Morris, S.L., Foltz, C.B., Hewett, P.C., 1991, *Astrophys. J.*, 373, 23
- Whittle, M., 1985, *MNRAS*, 213, 1 and 33
- Whittle, M., 1988, *MNRAS*, 216, 817
- Wills, B.J., Brotherton, M.S. & Fang, D., 1993, *Astrophys. J.*, 415, 563
- Wills, B.J. & Brotherton, M.S., 1996, preprint
- Wilson, A.S., Heckman, T.M., 1985, *Astrophysics of Active Galaxies and QSOs*, ed. J.S. Miller, p. 39
- Wilson, A., Ward, M. & Haniff, C., 1988, *Astrophys. J.*, 334, 121
- Wilson, A., 1991, *Physics of Active Galactic Nuclei*, eds. W.J. Duschl, S.J. Wagner, Springer Verlag, p. 307
- Woltjer, L., 1990, *Active Galactic Nuclei*, p. 1, Swiss Society for Astrophysics and Astronomy, eds. R.D. Blandford, H. Netzer, L. Woltjer, Springer Verlag
- Yaqoob, T. & Warwick, 1991, *MNRAS*, 248, 773
- Yaqoob, T. Warwick, R. S., Makino, F., Otani, C., Sokoloski, J.L., Bond, I.A., & Yamauchi, M., 1993, *MNRAS*, 262, 435
- Yee, H.K.C. & Oke, J.B., 1981, *Astrophys. J.*, 248, 472
- Zheng, W., 1996, *Astron. J.* preprint